BULLETIN OF THE POLISH ACADEMY OF SCIENCES
TECHNICAL SCIENCES, Vol. 67, No. 3, 2019
DOI: 10.24425/bpasts.2019.129644

INVITED PAPER

Coherent structures and flow control: genesis and prospect

M. GAD-EL-HAK*

Department of Mechanical & Nuclear Engineering, Virginia Commonwealth University, Richmond, VA 23284, USA

Abstract. The genesis of both coherent structures and reactive flow control strategies is explored. Futuristic control systems that utilize microsensors and microactuators together with artificial intelligence to target specific coherent structures in a transitional or turbulent flow are considered. Of possible interest to the readers of this journal is the concept of smart wings, to be briefly discussed early in the article.

Key words: smart wings, coherent structures, reactive flow control, adaptive control, machine-learning control, futuristic control systems, microsensors, microactuators, artificial intelligence, turbulent shear flows, history of flow control, history of coherent structures.

Chapter I: The period

It was the best of times, it was the worst of times, it was the age of wisdom, it was the age of foolishness, it was the epoch of belief, it was the epoch of incredulity, it was the season of Light, it was the season of Darkness, it was the spring of hope, it was the winter of despair, we had everything before us, we had nothing before us, we were all going direct to Heaven, we were all going direct the other way—in short, the period was so far like the present period, that some of its noisiest authorities insisted on its being received, for good or for evil, in the superlative degree of comparison only.

(Opening paragraph in *A Tale of Two Cities*
by Charles Dickens, 1859.)

1. Introduction

The ability to manipulate a flowfield actively or passively to effect a desired change is of great technological importance, and this may account for the fact that scientists and engineers pursue the subject more than any other topic in fluid mechanics. The potential benefits of realizing efficient flow-control systems include saving billions of dollars in annual fuel costs for land, air, and sea vehicles, reversing or at least slowing down dangerous global warming trends, and achieving economically and environmentally more competitive industrial processes involving fluid flows. Controlling a turbulent flow is particularly challenging, and this article provides an overview of that subject, although in the context of the broader field of flow control.

The genesis and interdependence of both coherent structures and reactive flow control strategies are explored in this survey. Especially for the uninitiated, the article is a modest attempt to guide through the bewildering complexity of nonlinear control strategies. Futuristic control systems that utilize microelectromechanical systems (MEMS) together with artificial intelligence/machine-learning control (AI/MLC) to target specific coherent structures in a transitional or turbulent flow are considered. Of interest to the readers of this journal is the concept of smart wings, to be discussed briefly herein. The historical nature of the present article precludes adequate coverage of the most recent literature in closed-loop flow control. That monumental task is left to another occasion.

We start in Section 2 with a brief introduction to the concept of smart wings. The genesis of coherent structures and flow control are provided in Sections 3 and 4, respectively. Section 5 attempts to delineate the modern views of and the association between both subjects. Progress in closed-loop control during the last two decades is tracked in Section 6. Concluding remarks and prospects are given in the last section.

2. Adaptive wings

A wing is the primary lift-generating surface of heavier-than-air aircraft. Unlike fixed wings on manmade airplanes, flapping wings on birds and insects generate both lift and thrust. Adaptive wings—also known as smart, compliant, intelligent, morphing, controllable, and reactive wings—are lifting surfaces that can change their shape in flight to achieve optimal performance at different speeds, altitudes, and ambient conditions. There are

*e-mail: gadelhak@vcu.edu

Manuscript submitted 2018-06-08, revised 2018-08-31, initially accepted for publication 2018-09-24, published in June 2019.

different levels of sophistication, or intelligence, that can be imbued in a particular design. Smart materials, smart structures, and reactive flow control are the fields of study by means of which an adaptive wing can be conceived, designed, optimized, constructed, and operated.

In helicopters, rotors supply both lift and thrust, which allow the rotorcraft to take off and land vertically, to hover, and to fly forward, backward, and laterally. Whether the wing is rigidly attached to the fuselage for fixed-wing airplanes or rotating for helicopters, a primary design objective of such lifting surface is to optimize the lift-to-drag ratio, which is achieved by controlling the airflow around the wing. Other design objectives for the wing include improving maneuverability and minimizing vibrations and flow-induced noise. The wing can have a set design optimized for specific flight conditions, or it can change shape to conform to a variety of conditions. Chosen judiciously, minute dynamic changes in the wing's shape can, under the right circumstances, greatly affect the airflow and thus the aircraft's performance.

2.1. Flapping wings. An ornithopter is a device that flies by flapping wing. Vertebrate birds and invertebrate insects can fly by flapping their wings, thus generating both lift and thrust, with the latter not particularly needed in the gliding or soaring mode of flight. Birds have strong yet lightweight skeletons, while two insect groups, the dragonflies and the mayflies, have flight muscles attached directly to the wings. Those small insects can fly via the clap and fling mechanism of lift generation, also known as the Weis-Fogh mechanism named after the Danish zoologist Torkel Weis-Fogh [1, 2].

Man's dream of flying has its genesis in the ancient-Greek mythology of Icarus and his master-craftsman father Daedalus. The flight of Icarus using feathers and wax attached to his (flapping) arms didn't end well, hence the idiom "don't fly too close to the sun". The ancient Assyrians depicted a god flying in an ornithopter about 3,000 years ago. The first successful flight of a manned ornithopter took place in 1942. The ability of a sinusoidally plunging airfoil to produce thrust, known as the Knoller-Betz or Katzmayer effect, has been investigated experimentally and numerically by Jones et al. [3]. These authors, and later Jones & Platzer [4], provide a brief history of human's flapping wings and their limited successes. They offer the idea of using both a fixed wing followed by two flapping wings, in biplane formation, flapping counterphase. After a decade of experimental and numerical investigations, the patented biomorphic concept [5] has been successfully demonstrated on a 25-cm span span, radio-controlled micro air vehicle (MAV).

2.2. Superiority of biological adaptive wings. Flying insects and birds, through millions of years of evolution, can change the shape of their flapping wings, subtly or dramatically, to adapt to various flight conditions. The resulting performance and agility are unmatched by any manmade aircraft. For example, the dragonfly can fly forward and backward, turn abruptly and perform other supermaneuvers, hover, feed, and even mate while aloft (Fig. 1). Undoubtedly, its prodigious wings contributed to the survival of the species for around 300 million years.

Fig. 1. Male and female Cardinal Meadowhawk dragonflies following airborne mating. The male has towed the just-inseminated female to a pond and is dipping her tail in the water so she can deposit her eggs. Reprinted with permission, *The Press Democrat*, Santa Rosa, CA

Among human-produced flyers, the Wright brothers changed the camber of the outboard tip of their aircraft's wings to generate lateral or roll control (combined with simultaneous rudder action for banked turn), thus achieving in 1903 the first heavier-than-air, controlled flight. The R.B. Racer built by the Dayton Wright Airplane Company in 1920 allowed the pilot to change the wing's camber in flight using a hand crank. The wings of today's commercial aircraft contain trailing-edge flaps and leading-edge slats to enhance the lift, during the relatively low speeds of takeoff and landing, and ailerons for roll control, all engaged by the pilot via clumsy, heavy, and slow servomechanisms. To equalize the lift and prevent rolling in forward flight, the rotary wings of most helicopters are cyclically feathered to increase the pitch on the advancing blade and decrease it on the retreating blade.

While certain insect's wings are quite smart, human-designed ones are not very intelligent, yet. With few exceptions—MAV being one of them—the level of autonomous adaptability sought in research laboratories is some years away from routine field deployment. Intelligent control of the wing's shape involves embedded sensors and actuators with integrated control logic; in other words, the wing's skin is made out of smart materials. The sensors detect the state of the controlled variable, for example the wall shear stress, and the actuators respond to the sensors' output based on a control law to effect the desired in-flight metamorphosing of the wing. For certain control goals, for example reduction of skin-friction drag, required changes in

the wing's shape can be microscopic. For others, for example morphing the wing for takeoff and landing, dramatic increases in camber may be needed.

2.3. Manmade smart wings. Adaptive wing design involves adding smart materials to the wing's structure and using these materials to effect flow changes. Smart materials are those that undergo transformations in one or more properties through physical interactions or external stimuli, such as stress, temperature, moisture, pH, or electric or magnetic fields. Such materials sense changes in their environment and adapt according to a feedforward or feedback control law (respectively, open-loop or closed-loop control). Smart materials include piezoelectrics, electrostrictors, magnetostrictors, shape-memory alloys, electrorheological and magnetorheological fluids, optical fibers, pH-sensitive polymers, temperature-responsive polymers, halochromic materials, chromogenic systems, non-Newtonian fluids, ferrofluids, photomechanical materials, and self-healing materials [6–8]. For no rational reason but rather customary usage, several other types of sensors and actuators that fall outside those categories are not usually classified as constituting elements of smart structures.

The piezoelectric effect is displayed by many noncentrosymmetric ceramics, polymers, and biological systems. The direct effect denotes the generation of electrical polarization in the material in response to mechanical stress. The poled material is then acting as a stress or strain sensor. The converse effect denotes the generation of mechanical deformation upon the application of an electrical charge. In this case, the poled material is acting as an actuator. The most widely used piezoceramic and piezopolymer are, respectively, lead zirconate titanate (PZT) and polyvinylidene fluoride (PVDF). Piezoelectrics are the most commonly used type of smart materials and the only ones that can be used readily as both sensors and actuators [8].

Electrostrictive materials are dielectrics that act similarly to piezoelectric actuators, but the relation between the electric charge and the resulting deformation in this case is nonlinear. Examples of such materials are lead magnesium niobate (PMN) compounds, which are relaxor ferroelectrics. Magneto-strictive materials, such as Terfenol-D, are actuators that respond to a magnetic field instead of an electric field.

Shape memory alloys, such as a nickel-titanium alloy known as Nitinol, are metal actuators that can sustain large deformation and then return to their original shape by heating without undergoing plastic deformation. Electrorheological and magnetorheological fluids rapidly increase in viscosity—by several orders of magnitude—when placed in, respectively, electric or magnetic fields. Both kinds of fluids can provide significant actuation power and are therefore considered for heavy-duty tasks such as shock absorbing for large-scale structures. Finally, optical fibers are sensors that exploit the refractive properties of light to sense acoustical, thermal, or mechanical-strain perturbations.

Outstanding issues to be resolved before smart materials for aircraft wings become routine include cost, complexity, weight penalty, maintenance, reliability, robustness, integrity of the structure on which the sensors and actuators are mounted, and finally current limitations on computer's memory, speed, and software. Sensors and actuators that have length scales between 1 and 1,000 micrometer constitute a special domain of smart materials that in turn is a cornerstone of microelectromechanical systems (MEMS). Several of the concepts discussed in this section will be revisited in Sections 4 and 5.

3. Coherent structures

The relatively recent realization that organized structures play an important role in all turbulent shear flows leads quite naturally to the concept of turbulence control via direct interference with these deterministic events. Active, predetermined, open-loop control can be employed, but perhaps much more effectively reactive control can be used where specific coherent structures are sensed then targeted for modulation to achieve a useful end result such as drag reduction, lift enhancement, mixing augmentation, and noise suppression. Reactive control strategies require sensors, actuators, and appropriate control algorithms as will be discussed in Sections 4 and 5, but for the present section we provide a gentle introduction to the fascinating world of coherent structures in transitional and turbulent flows. First, we briefly describe the different historical perspectives of turbulence. Secondly, we define what is meant by organized motions. This is followed by a summary of what is known about coherent structures in free-shear flows. Lastly, the important topic of coherent motions in wall-bounded flows is covered.

3.1. The changing paradigms of turbulence. Turbulence is the last great unsolved problem of classical physics. Or so it goes for a quote variously attributed to one of the great modern physicists: Albert Einstein, Richard Feynman, Werner Heisenberg, and Arnold Sommerfeld. But in fact the closest sentiments to this quote that could be traced are due to the classical physicist Horace Lamb [9] who, starting the second edition of his celebrated book *Hydrodynamics*, wrote under the heading of Turbulent Motion: "It remains to call attention to the chief outstanding difficulty of our subject." No one knows how to obtain stochastic solutions to the well-posed set of partial differential equations that governs turbulent flows. Averaging those nonlinear equations to obtain statistical quantities always leads to more unknowns than equations, and ad hoc modeling is then necessary to close the problem. So, except for a rare few limiting cases, first-principles analytical solutions to the turbulence conundrum are not possible. In the words of John Lumley [10], "Turbulence is a difficult problem that is unlikely to suddenly succumb to our efforts. We should not await sudden breakthroughs and miraculous solutions, but rather keep at it slowly building one small brick at a time."

Our struggle to conquer turbulence has been long and arduous. Lots of sweat, few victories, and much frustration. Not surprisingly, the way turbulence is being viewed as a complex physical phenomenon has changed over the years. Indeed, key ideas in the field continue to rise and fall [11], and perhaps even to rise again! We now know that turbulence is random fluctuations superimposed on mean flow. A turbulent flow con-

tains motions with numerous time- and length-scales, which are random in the sense that there is zero probability of any flow variable having a particular value and there is zero energy in any one particular frequency or wavenumber. In other words, both the probability density function and spectrum of any flow variable are continuous and finite [12]. But we also know that the seemingly random mess is at least in part deterministic: a combination of coherent and incoherent motions.

Historically, there are perhaps five doctrines in approaching the five-century-old conundrum: visualization; first principles; statistical approach; coherent structures; and modern tools. Each of these dogmas is described in turn in the following five sub-subsections.

3.1.1. Visualization. Perhaps more than any other tool available to tackle the problem of fluid mechanics in general and turbulence in particular, flow visualization is singly responsible for many of the most exciting discoveries in the field. Relatively simple, quick, and capable of giving both global and local behavior, rendering the fluid motion accessible to visual perception can yield invaluable qualitative as well as quantitative information about a complex flow. However, one has to be extremely vigilant to avoid the many possible pitfalls when interpreting visual images of fluid flows, particularly time-dependent flows [13].

Leonardo da Vinci pioneered the visualization genre more than 500 years ago. Much of Leonardo's notebooks of engineering and scientific observations were translated into English in a magnificent two-volume book by Edward MacCurdy [14]. Succinct descriptions of the smooth and eddying motions of water alone occupy 121 pages. In there, one can easily discern the Renaissance genius's prophecy of some of the turbulence physics to be discovered centuries after his time. Particularly relevant to the subject of coherent structures, the words eddies and eddying motions percolate throughout Leonardo's treatise on liquid flows.

Figure 2 is perhaps the world's first use of visualization as a scientific tool to study a turbulent flow. Around 1500, Leonardo sketched a free water jet issuing from a square hole into a pool. He wrote, "Observe the motion of the surface of the water, which resembles that of hair, which has two motions, of which one is caused by the weight of the hair, the other by the direction of the curls; thus the water has eddying motions, one part of which is due to the principal current, the other to the random and reverse motion." [Translated] Reflecting on this passage, Lumley [15] speculates that Leonardo da Vinci might have prefigured the now famous Reynolds turbulence decomposition nearly 400 years prior to Osborne Reynolds's flow visualization and analysis.

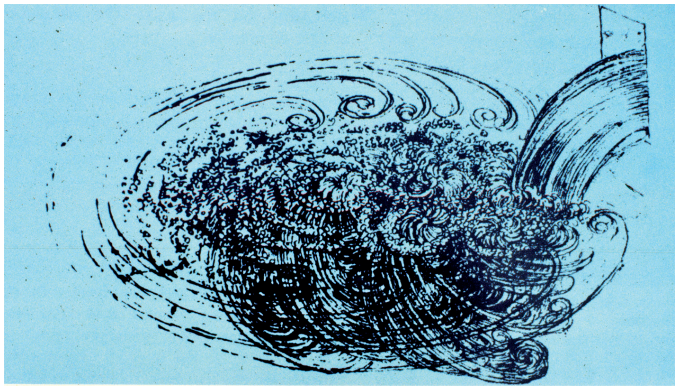

Fig. 2. Leonardo da Vinci's sketch of water exiting from a square hole into a pool; circa 1500. Royal Collection Trust; www.royalcollection.org.uk/collection/themes/exhibitions/royal-gifts/buckingham-palace/hm-queen-elizabeth-ii

In describing the swirling water motion behind a bluff body, da Vinci provided the earliest reference to the importance of vortices in fluid motion: "So moving water strives to maintain the course pursuant to the power which occasions it and, if it finds an obstacle in its path, completes the span of the course it has commenced by a circular and revolving movement." [Translated] Leonardo accurately sketched the pair of quasi-stationary, counter-rotating vortices in the midst of the random wake.

Finally, da Vinci's words "… the small eddies are almost numberless, and large things are rotated only by large eddies and not by small ones, and small things are turned by both small eddies and large," presage Richardson's cascade, coherent structures, and large-eddy simulations, at least.

3.1.2. First principles. At the time of Leonardo da Vinci, neither calculus nor the laws of mechanics were available, of course. Little more than a century and half after the incomparable Isaac Newton's *Philosophiæ Naturalis Principia Mathematica* was published in 1687, the first principles of viscous fluid flows were firmed in the form of the Navier–Stokes equations, with major contributions by Navier in 1823, Cauchy in 1828, Poisson in 1829, Saint Venant in 1843, and Stokes in 1845. With very few exceptions, the Navier–Stokes equations provide an excellent model for both laminar and turbulent flows. But in the latter case no analytical solutions are possible for several reasons: (i) the governing partial differential equations are nonlinear; (ii) the dependent variables are random functions of space and time; and (iii) the usual simplifications and symmetries do not apply to the instantaneous, three-dimensional flow quantities (although they *may* apply to statistical quantities). So, even though the turbulence problem is well defined mathematically, no one can analytically integrate the equations of motion, or for that matter do much with them when dealing with stochastic phenomena.

For a century and half only laminar flows and their (mostly linear) stability were tractable analytically. Recent advances in computer power made it possible to return to first principles in the case of a turbulent flow and numerically integrate the Navier–Stokes equations for simple geometries and rather low Reynolds numbers. Notwithstanding their rather severe restrictions and limitations, direct numerical simulations (DNS) are therefore the only route available for a direct, brute-force onslaught on the turbulence problem. On the other hand, raw numerical solutions overwhelm the senses with data while providing little physical understanding.

3.1.3. Statistical view of turbulence. As is clear from the previous subsubsection, up until recently not much could be done

with first principles for the turbulence problem. But do we really need the kind of detailed information that DNS provides for all the random flow variables? Would a statistical description yielding such quantities as mean or root-mean-square values, correlation functions, spectra, and probability distributions suffice? The answer is an emphatic yes, but there is a price to pay for the lowered expectations.

Based on a painstaking flow visualization study, Osborne Reynolds [16] made the observation that a pipe flow is either direct or sinuous (laminar or turbulent) depending on the value of a dimensionless parameter, which we now call the Reynolds number. Eleven years later, on 24 May 1894, Reynolds read to an audience of the British Royal Society a follow-up paper in which he provided a physical explanation for his earlier observation. That second treatise, published in 1895, is considered by many to pioneer the modern scientific approach to the turbulence problem and even to reshape the direction of fluid mechanics research in general for the next century. Reynolds [17] ascertained that a turbulent flow field can be decomposed into mean and fluctuating parts. He thus was able to write expressions for the time-averaged momentum, now known as the Reynolds-averaged Navier–Stokes (RANS) equations, in which convective stress terms appear as new unknowns. This was the dawn of the statistical doctrine of turbulence research. Reynolds [17] derived also the transport equation for the turbulence kinetic energy, and demonstrated that the apparent stresses due to turbulence interacting with the mean velocity gradient lead to a transfer of kinetic energy from the mean motion to the turbulent motion.

In the statistical approach, a temporal, spatial, or ensemble average is defined and the equations of motion are written for the various moments of the fluctuations about this mean. Unfortunately, the nonlinearity of the Navier–Stokes equations guarantees that the process of averaging to obtain moments results in an open system of equations, where the number of unknowns is always greater than the number of equations, and more or less heuristic modeling is used to close the equations. This is known as the closure problem, and again makes obtaining rational solutions to the (averaged) equations of motion impossible.

Attempts to close the RANS equations are at the heart of the turbulence modeling community. From the simple mixing length ideas of Prandtl, Taylor, and von Kármán to the more involved Reynolds-stress, or second-order, modeling and beyond, a whole new industry sprang out of the Reynolds decomposition [18–21].

3.1.4. Reemergence of coherent structures. The recognition of coherent structures during the last few decades brought us back a full circle to the time of Leonardo. Not only was visualization once again the method of choice for the major discoveries but also was the re-affirmation of the importance of eddying motions and the co-presence of large, organized motions and small, random ones. In the view of Hussain [22], the search for coherent events is the embodiment of human's desire to find order in apparent disorder.

The modern history of coherent structures is amply chronicled in the article by Liu [23]. He asserts that the kernel idea germinated as a result of a discussion that took place during the *Fifth International Congress for Applied Mechanics* held in Cambridge, Massachusetts, 12–16 September 1938. There, both Tollmien and Prandtl, responding to a comment by von Kármán regarding the difficulties of reconciling a scalar mixing length with turbulence measurements made in a channel, suggested that the measured turbulence fluctuations include both random and non-random elements. Dryden [24] pointed out that the boundary layer measurements conducted at a later date at the U.S. National Bureau of Standards supported the ideas of Tollmien and Prandtl. Dryden also lamented that there is no known procedure, experimental or theoretical, that can be used to separate the random processes from the non-random ones.

Liepmann [25], citing measurements in free-shear turbulent flows, in flows between rotating cylinders, and in the far-wake of bluff bodies, emphasized the importance of the presence of secondary, large-scale structures superimposed upon the primary turbulent shear flow. Townsend [26] thoroughly exploited this concept in the first edition of his famed monograph on the structure of turbulent shear flows. He recognized the quasi-deterministic nature of large eddies, and inferred their shapes from the long-time-averaged spatial-correlation tensor measured in an Eulerian frame. Nevertheless, Townsend's approach suffers from a number of shortcomings, including the lack of a unique relationship between the correlation tensor and the unsteady flow that produces it. Lagrangian approaches offer a more objective characterization of vortices, saddle points, etc. [27, 28], and, particularly for transient flows, so does discrete Morse topology [29].

In a later paper, Liepmann [30] once again underscored the splitting of seemingly random fluctuations into large-scale, deterministic structures and fine-grained turbulence. Liepmann asserted the importance of large-scale structures in many technological problems in aerodynamic sound, combustion, etc. Liepmann [11] was perhaps the first to suggest that the existence of deterministic eddies in turbulent flows can be exploited for control purposes via direct interference with these large structures. This is the kernel idea behind reactive flow control, to be discussed in Sections 4 and 5.

The modern view of coherent structures resulted from flow visualization studies of low-Reynolds-number boundary layers conducted first at the University of Maryland then at Stanford University during the late 1950s and 1960s. The new doctrine did not pick up steam, however, until the milestone discovery of Brown and Roshko [31, 32] of organized motions in a mixing layer at Reynolds numbers far exceeding transitional ones. The large spanwise vortices, prominent in visual images of the shear layer, were totally missed in the correlation studies of Townsend and others.

3.1.5. Latest tools. Finally, dynamical systems and wavelets are the modern tools to tackle the last conundrum. A turbulent flow is a complex, nonlinear dynamical system, which, at high Reynolds numbers, has an infinite number of degrees of freedom. The issue here is the possibility of representing such a system with a 'reasonable' number of degrees of freedom. A Fourier decomposition would not do since it requires a very large number of components.

Mechanical systems with three or more degrees of freedom are capable of chaotic behavior exemplified by a strange attractor in phase space. Such systems are complex, aperiodic, random, and display extreme sensitivity to initial conditions, but are nevertheless still deterministic. The book by Holmes et al. [33] provides an excellent introduction to the dynamical systems approach to tackle the turbulence problem.

Under rather severe restrictions, chaos theory allows the representation of turbulence as a low-dimensional dynamical system. The flow is modeled as coherent structures plus a parameterized turbulent background. The proper orthogonal decomposition, or Karhunen-Loève decomposition, has been of great utility because it is capable of representing the flow with minimum number of modes. Such representation is useful on two fronts: (i) providing an inexpensive—as compared to DNS—surrogate to the turbulent flow and in the process shedding light on its basic physics; and (ii) once the flow is successfully represented as a dynamical system with a reasonably small number of degrees of freedom, chaos control concepts can be utilized to achieve effective manipulation with minimum energy expenditure.

The dynamical system approach thus far has been successful for flows near transition or near a solid wall, in which cases the associated low Reynolds number implies that a relatively small number of degrees of freedom is excited and that a large fraction of the energy is in the ordered, deterministic component of the flow. More and more degrees of freedom are excited as the flow moves farther from transition or away from the wall. In those cases, the structure of the strange attractor becomes so complex as to negate the dynamical system approach advantages over the classical statistical description.

The second modern tool is wavelets, introduced about three decades ago. Wavelet transform is used in many fields including signal processing, data compression, image coding, and numerical analysis [34]. The technique is based on group theory and square integrable representation in terms of basis functions, called wavelets, that are localized in both physical and wavenumber spaces. Farge's review article [35] provides a good introduction to the field and particularly its application to turbulence. A second paper by Vasilyev et al. [36] offers a gentle introduction to the use of wavelets for numerically solving complex, multi-scale partial differential equations.

Wavelets allow the unfolding of a flow field into both space and scale, and possibly even direction. Wavelets are localized analyzing functions that are dilated or contracted prior to convolving with the signal under consideration to achieve scale decomposition. Wavelet analysis can be viewed as a multi-level or multi-resolution representation of a function, each level of resolution consisting of basis functions that have the same scale but are located at different positions. In contrast to Fourier transform, wavelet transform is a local one with the behavior of the signal at infinity playing no role in the analysis. Continuous wavelet transforms offer redundant unfolding in terms of space and scale, and are thus suited for tracking coherent motions and their contributions to the energy spectrum. Discrete wavelet transforms, on the other hand, allow orthonormal projection on a minimal number of independent modes, and may thus be used to model the flow dynamics.

Basis functions such as Mexican-hat wavelets or Daubechies scaling functions can be used to decompose a velocity field into eddies. Since coherent structures are always of limited spatial extent, wavelet decomposition seems to be a better representation of them than, say, Fourier representation. Fourier modes in the form of (space-filling) trigonometric functions stretch off to infinity, and are thus suited for decomposing a velocity field into waves of different, independent wavelengths. On the other hand, a limited-extent eddy is ideally represented by modes that act in groups as the wavenumber increases. Wavelets offer complete representation at least for homogeneous turbulence. (As do a variety of conventional techniques with varying degrees of computational efficiency and accuracy.) For inhomogeneous flows, a complete representation using wavelets is not as readily achieved and some difficulties remain to be resolved. Nevertheless, the technique offers some potential advantages from the point of view of controlling turbulent flows. Specifically, wavelet transforms may be used as an efficient, unbiased strategy for real-time identification of coherent structures from an instantaneous velocity signal, say. This step is of course at the heart of effective reactive control.

3.2. What is a coherent structure? The statistical view that turbulence is essentially a stochastic phenomenon having a randomly fluctuating velocity field superimposed on a well-defined mean has been changed in the last few decades by the realization that the transport properties of all turbulent shear flows are dominated by quasi-periodic, large-scale vortex motions [37–40]. Despite the extensive research work in this area, no generally accepted definition of what is meant by coherent motion has emerged. In physics, coherence stands for well-defined phase relationship. We provide here two rather different views, the first is general and the second is more restrictive. According to Robinson [41], a coherent motion is defined as a three-dimensional region of the flow over which at least one fundamental flow variable (velocity component, density, temperature, etc.) exhibits significant correlation with itself or with another variable over a range of space and/or time that is significantly larger than the smallest local scales of the flow. The rather restrictive definition is given by Hussain [22]: a coherent structure (CS) is a connected turbulent fluid mass with instantaneously phase-correlated vorticity over its spatial extent. In other words, underlying the random, three-dimensional vorticity that characterizes turbulence, there is a component of large-scale vorticity that is instantaneously coherent over the spatial extent of an organized structure. The apparent randomness of the flow field is, for the most part, due to the random size and strength of the different types of organized structures comprising that field. Several other definitions are catalogued by Delville et al. [42]. The same authors also provide a cookbook-style approach to coherent structure identification using a variety of classical and modern strategies.

The challenge is to identify a coherent structure well hidden in a sea of random background, when such a structure is present either in a visual impression of the flow or in an instantaneous velocity, temperature, or pressure signal. This is of course not a trivial task, although it is at the heart of reactive flow control

strategies. Complicating the issue is that coherent structures change from one type of flow to another and even in the same type of flow as initial and boundary conditions vary. The largest eddies are of the same scale as that of the flow, and consequently cannot be universal. Identifying a coherent structure based on certain dynamical properties is more likely to succeed, but is quite involved. On the other hand, a kinematic detector—based on the perception of its creator—of the dynamic behavior of the organized motion is simpler to employ but runs the risk of detecting the presence of non-existent objects [43, 44]. Benefiting from hindsight, the few flow visualization pictures depicted in the next two subsections may help exploring the nature of the whole beast. We first discuss coherent structures in free-shear flows, followed by the all important CS in wall-bounded flows.

3.3. Free-shear flows. As indicated above, there is no universal coherent structure. Organized motions in wakes are different from those in boundary layers. In a jet issuing from a nozzle with thin, laminar boundary layer on its inner surface, coherent structures are easily observed, while a jet issuing from a nozzle with thick, turbulent boundary layer has organized structures that are nearly undetectable. In general, the proportion of readily detectable organized turbulence decreases with the level of disturbances in the incoming flow.

In general again, coherent structures in free-shear flows are easier to detect and characterize than those in wall-bounded flows. According to Liu [23], for free-shear turbulent flows it is not necessary to conjecture that the local fine-grained turbulence rearranges itself to give bursts of white noise in order to maintain the hydrodynamically unstable waves, as is the case for wall-bounded flows. The existence of large-scale, coherent motions in mixing layers, jets, and wakes is instead a manifestation of the dynamic instability associated with the local inflectional mean-velocity profiles. As a result, free-shear flows have pronounced organized motions and wave-like structures [40, 45].

In a mixing layer, for example, the dominant structures are roller-like vortices as large as the shear layer itself [31, 32, 46]. The growth of the mixing layer results from the amalgamation of neighboring large eddies rather than from their individual growth [47]. The large transverse eddies in a mixing layer are strung together by a spaghetti-like net of smaller-scale, streamwise, counter-rotating vortices. If the mixing layer develops from undisturbed conditions (i.e., thin, laminar boundary layers on the splitter plate), the roller-like vortices are energetic and only relatively slowly become three-dimensional and less organized. If, on the other hand, the splitter plate has thick, turbulent boundary layers, the proportion of organized motion is considerably less dominant.

The spark-shadowgraph photograph in Fig. 3 depicts the mixing of a fast-moving stream of helium (top) and a slower stream of nitrogen (bottom), both moving from left to right. The two streams have the same mean momentum per unit cross-sectional area, $\rho_1 \overline{U}_1^2 = \rho_2 \overline{U}_2^2$, and originate from a splitter plate with laminar boundary layers. The roller-like vortices convect at nearly constant speed equal to the average $\frac{1}{2}(\overline{U}_1 + \overline{U}_2)$. Increasing the Reynolds number produces more small-scale structures without significantly altering the large eddies.

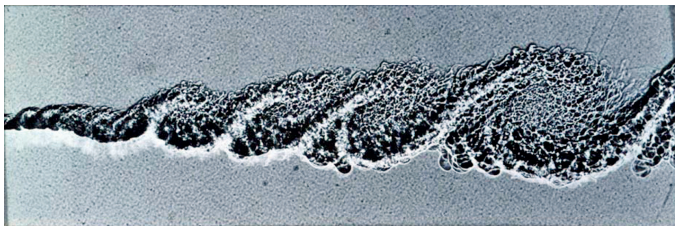

Fig. 3. High-Reynolds-number mixing layer. The helium stream on top moves at a velocity of 10 m/s, and the nitrogen stream on bottom moves at a speed of 3.78 m/s. The whole test section is pressurized to $\overline{P} = 8$ atm, giving a Reynolds number based on downstream distance of the order of 10^6. From Brown and Roshko [32]

The spanwise vortices remain as a permanent dominant feature even at high Reynolds numbers. Brown and Roshko's experiment [31, 32] is important because it was the first to show a significant proportion of organized turbulence even at Reynolds numbers far from transitional ones. Moreover, a much closer tie between stability and turbulence has been established: the essentially two-dimensional vortices in the fully-turbulent flow are clearly related to the general instability modes of a simple vortex sheet.

The organized structures in jets are not as dominant as those in mixing layers having similar levels of disturbances in the incoming flow. Also, in contrast to mixing layers, the spanwise vortices shed in the wake of bluff bodies do not pair. The basic mechanism for wake growth is entrainment.

3.4. Wall-bounded flows. We now turn our attention to the more enigmatic boundary layers and channel flows. In a wall-bounded flow, a multiplicity of coherent structures have been identified mostly through flow visualization experiments, though some important early discoveries have been made using correlation measurements [48–50]. Although the literature on this topic is vast, no research-community-wide consensus has been reached particularly on the issues of the origin of and interaction between the different structures, regeneration mechanisms, and Reynolds number effects. What follow are somewhat biased remarks addressing those issues. At times diverse view points will be presented but for the most part particular scenarios, which in my opinion are most likely to be true, will be emphasized. The interested reader is referred to the book edited by Panton [51], which emphasizes the self-sustaining mechanisms of wall turbulence, and the large number of review articles available [37, 39–42, 52–58]. The paper by Robinson [41] in particular summarizes many of the different, sometimes contradictory, conceptual models offered by different research groups. Those models are aimed ultimately at explaining how the turbulence maintains itself, and range from the speculative to the rigorous, but unfortunately none is self-contained and complete. Furthermore, the structure research dwells largely on the kinematics of organized motion and less attention is given to the dynamics of the regeneration process, an important element for effective reactive flow control.

3.4.1. Overview. With few exceptions, most of the available structural information on wall-bounded flows come from rather low-Reynolds-number experiments and numerical simulations. Organized structures appear to be similar in all wall-bounded flows only in the inner layer. The outer region of a boundary layer is by necessity different from the core region of a pipe or channel flow. An overall view, whose source of information is predominately low-Reynolds-number experiments, is presented here. As will become clear throughout the discussion, the picture that emerges at high Reynolds numbers is quite different, and structural information gleaned from low-Reynolds-number physical and numerical experiments may not be very relevant to the more practically important high-Reynolds-number flows.

In boundary layers, the turbulence production process is dominated by three kinds of quasi-periodic eddies: the large outer structures, the intermediate Falco eddies, and the near-wall eddies. Examples of these coherent structures visualized in laboratory-scale boundary layers are depicted in Figs. 4–6. Laser sheet illumination is used in all three photographs. The large eddies forming on a flat plate towed in a water channel are seen in the side view in Fig. 4. The flow (relative to the towed plate) is from left to right. The artificially tripped boundary layer has a momentum thickness Reynolds number at the observation station of $\Re_\theta \equiv U_\infty \delta_\theta / \nu = 725$, and is marked with fluorescent dye.

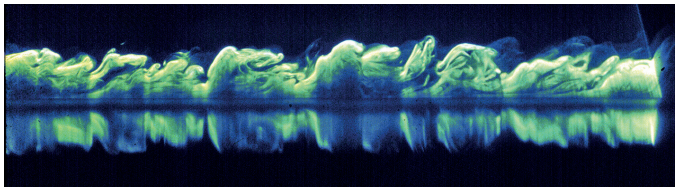

Fig. 4. Side view of a low-Reynolds-number turbulent boundary layer, $\Re_\theta = 725$. Flat plate towed in a water tank. Large eddies are visualized using a sheet of laser and fluorescent dye. From Gad-el-Hak et al. [59]

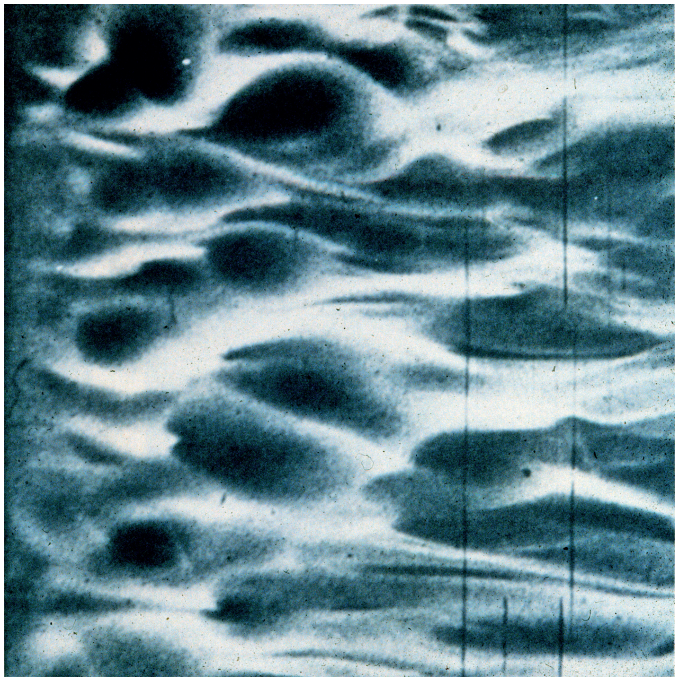

Fig. 5. Top view of a low-Reynolds-number turbulent boundary layer, $\Re_\theta = 742$. Wind tunnel experiment. Pockets, believed to be the fingerprints of typical eddies, are visualized using dense smoke illuminated with a sheet of laser. From Falco [60]

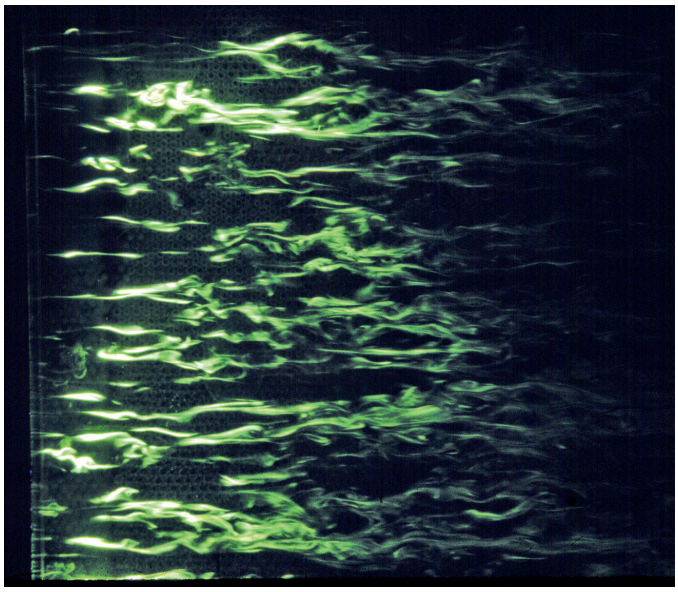

Fig. 6. Top view of a low-Reynolds-number turbulent boundary layer, $\Re_\theta = 725$. Flat plate towed in a water tank. Low-speed streaks are visualized using a sheet of laser and fluorescent dye. From Gad-el-Hak et al. [59]

A smoke-filled boundary layer shown in top view in Fig. 5 depicts the characteristic pockets believed to be induced by the motion of Falco's eddies over the wall [60]. Falco's experiments were conducted in a wind tunnel at a Reynolds number of $\Re_\theta = 742$, and the boundary layer was again artificially tripped.

Finally, the top view in Fig. 6 depicts the low-speed streaks in the near-wall region of the same turbulent boundary layer previously shown in side view in Fig. 4. Flow direction is again from left to right, and the thin sheet of laser used for illumination is parallel to and almost touching the wall.

Figure 7, from Gad-el-Hak et al. [44], shows a top view of an artificially-generated turbulent spot evolving in a laminar

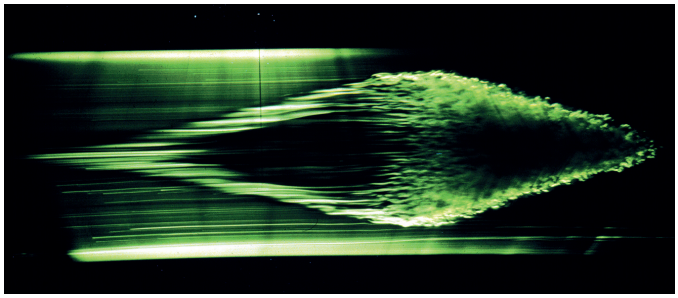

Fig. 7. Top view of an artificially-generated turbulent spot evolving in a laminar boundary layer. The dispalcement thickness Reynolds number at the spot's initiation point is $\Re_{\delta^*} = 625$. From Gad-el-Hak et al. [44]

boundary layer. The displacement thickness Reynolds number at the spot's initiation point is 625, well above the critical $\Re_{\delta^*}$ for linear instability. Laser-induced fluorescence is used to visualize different cuts through the growing turbulent structure. In this figure, the laser sheet is parallel to and very near the flat wall. The dynamics within the spot appear to be controlled by many individual eddies, similar to those within a fully-developed turbulent boundary layer. The spot grows in the spanwise direction by an efficient mechanism, which Gad-el-Hak et al. [44] termed *growth by destabilization* process. Near the edges of the spot, the dye lines are sharp, indicative of the initial breakdown into chaotic motion. Toward the middle, on the other hand, the dye becomes more diffused because the turbulence there is older and more mixing has taken place [61].

In a turbulent boundary layer, the large, three-dimensional bulges (Fig. 4) scale with the layer thickness, δ, and extend across the entire boundary layer [62, 63]. These eddies control the dynamics of the boundary layer in the outer region, such as entrainment, turbulence production, etc. The large eddies are characterized by a sharp interface and a highly contorted surface that exhibits a significant amount of folding [64] and has a fractal dimension of close to 2.4 [65]. They appear randomly (quasi-periodically) in space and time, and seem to be, at least for moderate Reynolds numbers, the residue of the transitional Emmons spots [44, 61, 66]. Note, however, that at higher Reynolds numbers ($\Re_\theta > 5{,}000$) the very existence of the large eddy as an isolated coherent structure has been questioned by Head and Bandyopadhyay [67].

The Falco eddies are also highly coherent and three-dimensional. Falco named them 'typical eddies' because they appear in wakes, jets, Emmons spots, grid-generated turbulence, and boundary layers in zero, favorable, and adverse pressure gradients [68, 69]. They have an intermediate scale of about 100 wall units. The Falco eddies appear to be an important link between the large structures and the near-wall events. In plane view using smoke visualizations, smoke fills the near-wall region of a boundary layer and the roughly circular regions devoid of marked fluid are called pockets. These undulations are very similar to the so-called folds observed by Perry et al. [70]. Falco [60] asserts that the pockets are the 'footprints' of some outer structures that induce fluid toward the wall. Robinson et al. [71] analyzed the database generated from the direct numerical simulations of Spalart [72, 73]. They concur that the pockets are the signature of local wall-ward motions, evidenced by spanwise divergence of streamlines above regions of high wall-pressure. Low-pressure regions, on the other hand, occur along lines of converging streamlines associated with outward motion. Those motions are, respectively, the sweeps and ejections events.

In the wall region, viscous forces dominate over inertial ones. The characteristic scales there are obtained from the magnitude of the mean vorticity in the region and its viscous diffusion away from the wall. Thus, the viscous time-scale, t_ν, is given by the inverse of the mean wall vorticity

$$t_\nu = \left[\left.\frac{\partial \bar{U}}{\partial y}\right|_w\right]^{-1} \tag{1}$$

and the viscous length-scale, ℓ_ν, is determined from the characteristic distance by which the (spanwise) vorticity is diffused from the wall, and is thus given by

$$\ell_\nu = \sqrt{\nu t_\nu} = \sqrt{\frac{\nu}{\left.\frac{\partial \bar{U}}{\partial y}\right|_w}} \tag{2}$$

where ν is the kinematic viscosity. The wall velocity scale (so-called friction velocity, u_τ) follows directly from the time- and length-scales

$$u_\tau = \frac{\ell_\nu}{t_\nu} = \sqrt{\nu \left.\frac{\partial \bar{U}}{\partial y}\right|_w} = \sqrt{\frac{\tau_w}{\rho}} \tag{3}$$

where τ_w is the shear stress at the wall, and ρ is the fluid density. A wall unit implies scaling with the viscous scales, and the usual $()^+$ notation is used; for example, $y^+ = y/\ell_\nu = y u_\tau/\nu$.

The third kind of eddies exists in the wall region ($0 \leq y^+ \leq 100$) where the Reynolds stress is produced in an intermittent fashion. At typical laboratory Reynolds numbers, half of the total production of turbulence kinetic energy $\left(-\overline{uv}\,\partial \bar{U}/\partial y\right)$ takes place near the wall in the first 5% of the boundary layer (smaller fraction of the boundary layer thickness at higher Reynolds numbers), and the dominant sequence of intense organized motions there are collectively termed the bursting phenomenon. This dynamically significant process, identified during the 1960s by researchers at Stanford University [74–79], was reviewed by Willmarth [53] and Blackwelder [80], and relatively more recently by Blackwelder [58].

The bursting process, according to at least one school of thought, begins with elongated, counter-rotating, streamwise vortices having diameters of approximately 40 wall units or $40\nu/u_\tau$. The estimate for the diameter of the vortex is obtained from the conditionally-averaged spanwise velocity profiles reported by Blackwelder and Eckelmann [81]. There is a distinction, however, between vorticity distribution and a vortex [41, 71, 82], and the visualization results of Smith and Schwartz [83] may indicate a much smaller diameter. In any case, the counter-rotating vortices exist in a region of strong shear and induce low- and high-speed regions between them. Those low-speed streaks were first visualized by Francis Hama at the University of Maryland—see Corrsin [84]—although Hama's contribution is frequently overlooked in favor of the subsequent and more thorough studies conducted at Stanford University and cited above. The vortices and the accompanying eddy structures occur randomly in space and time. However, their appearance is sufficiently regular that an average spanwise wavelength of approximately 80 to $100\nu/u_\tau$ has been identified by Kline et al. [76] and numerous others.

It might be instructive at this point to emphasize that the distribution of streak spacing is very broad. The standard deviation is 30–40% of the more commonly quoted mean spacing between low-speed streaks of 100 wall units. Both the mean and standard deviation are roughly independent of Reynolds

number in the relatively limited range of reported measurements [85, 86], $\Re_\theta = 300$–$6{,}500$. Butler and Farrell [87] have shown that the mean streak spacing of $100\nu/u_\tau$ is consistent with the notion that this is an optimal configuration for extracting "the most energy over an appropriate eddy turnover time". In their work, the streak spacing remains 100 wall units at Reynolds numbers, based on friction velocity and channel half-height, of $a^+ = 180$–360.

Kim et al. [77] observed that the low-speed regions (Fig. 6) grow downstream, lift up, and develop (instantaneous) inflectional $U(y)$ profiles. According to Swearingen and Blackwelder [88], inflectional $U(z)$ profiles are just as likely to be found in the near-wall region and can also be the cause of the subsequent bursting events. At approximately the same time, the interface between low- and high-speed fluid begins to oscillate, apparently signaling the onset of a secondary instability. A low-speed region lifts up away from the wall as the oscillation amplitude increases, and then the flow rapidly breaks up into a completely chaotic motion. The streak oscillations commence at $y^+ \approx 10$, and the abrupt breakup takes place in the buffer layer although the ejected fluid reaches all the way to the logarithmic region. Since the breakup process occurs within a very short time-scale, Kline et al. [76] called that event a burst.

Virtually all of the net production of turbulence kinetic energy in the near-wall region occurs during these bursts. Corino and Brodkey [89] showed that the low-speed regions are quite narrow, $\approx 20\nu/u_\tau$, and may also have significant shear in the spanwise direction. They also indicated that the ejection phase of the bursting process is followed by a large-scale motion of upstream fluid that emanates from the outer region and cleanses (sweeps) the wall region of previously ejected fluid. The sweep phase is, of course, required by the continuity equation and appears to scale with outer-flow variables. The sweep event seems to stabilize the bursting site, in effect preparing it for a new cycle.

Considerably more has been learned about the bursting process during the last few decades. For example, Falco [60, 90, 91] has shown that when a typical eddy, which may be formed in part by ejected wall-layer fluid, moves over the wall it induces a high uv sweep (positive u and negative v). The wall region is continuously bombarded by pockets of high-speed fluid originating in the logarithmic and possibly the outer regions of the flow. These pockets appear to scale with wall variables—at least in the limited Reynolds number range where they have been observed, $\Re_\theta = \mathcal{O}[1{,}000]$—and tend to promote and enhance the inflectional velocity profiles by increasing the instantaneous shear leading to a more rapidly growing instability. The relation between the pockets and the sweep events is not clear, but it seems that the former forms the highly irregular interface between the latter and the wall-region fluid. More recently, Klewicki et al. [92] conducted a four-wire hot-wire probe measurements in a low-Reynolds-number canonical boundary layer to clarify the role of velocity–spanwise-vorticity interactions regarding the near-wall turbulent-stress production and transport.

Other significant experiments were conducted by Tiederman and his students [93–96], Smith and his colleagues [83, 97, 98], and the present author and his collaborators [99, 100]. The first group conducted extensive studies of the near-wall region, particularly the viscous sublayer, of channels with Newtonian as well as drag-reducing non-Newtonian fluids. Smith's group, using a unique, two-camera, high-speed video system, was the first to indicate a symbiotic relationship between the occurrence of low-speed streaks and the formation of vortex loops in the near-wall region. Gad-el-Hak and Hussain [99] and Gad-el-Hak and Blackwelder [100] have introduced methods by which the bursting events and large-eddy structures were artificially generated in an otherwise laminar boundary layer. Their experiments greatly facilitated the study of uniquely controlled simulated coherent structures via phase-locked measurements.

3.4.2. Open issues. There are at least four unresolved issues regarding coherent structures in wall-bounded flows, not all are necessarily independent: (i) how does a particular structure originate; (ii) how do different structures, especially the ones having disparate scales, interact; (iii) how does the turbulence continue to regenerate itself; and (iv) does the Reynolds number affect the different structures in any profound way? The primary difficulty in trying to answer any of those queries stems from the existence of two scales in the flow that become rather disparate at large Reynolds numbers. The closely related issues of origin, inner/outer interaction, and regeneration will be addressed in the following three subsubsections. The fourth issue, Reynolds number effects, is extensively discussed elsewhere [101, 102].

3.4.3. Origin of different structures. Faced with the myriad of coherent structures existing in the boundary layer, a legitimate question is where do they all come from and which one is dynamically significant? Sreenivasan [103] offers a glimpse of the difficulties associated with trying to answer this question. The structural description of a turbulent boundary layer may not be that complicated, however, and some of the observed structures may simply be a manifestation of the different aspects of a more basic coherent structure. For example, some researchers argue that the observed near-wall streamwise vortices and large eddies are, respectively, the legs and heads of the omnipresent hairpin vortices [67]. Nevertheless, that still leaves us with a minimum number of building blocks that must be dealt with.

If the large eddies are assumed to be dynamically significant, then how are they recreated? It is easy to argue that the conventional laminar-to-turbulence transition cannot be responsible, because the same large eddies appear even in strongly tripped boundary layers where the usual transition routes are by-passed. Wall events cannot be responsible for creating large eddies because of their extremely small relative-scale at high Reynolds numbers. Furthermore, no hierarchical amalgamation of scales has been observed to justify such proposition.

If, alternatively, wall events are assumed to dominate, then where do the streamwise vortices or the low-speed streaks come from and what mechanism sustains the bursting cycle? Mechanisms that assume local instability cannot be valid at high Reynolds numbers where the wall layer is, say, 0.1% of the boundary layer thickness, and it is difficult to conceive that 99.9% of the boundary layer has no active role in the generation and maintenance of turbulence. On the other hand, assuming that

the bursting events are triggered by the large eddies brings us back to the original question of where do the latter come from.

The above difficulties explain the lack of a self-consistent model of the turbulent boundary layer, despite the enormous effort expended to establish such model. None of the existing models is complete in the sense that none accounts for each aspect of the flow in relation to every other aspect. Adding to the difficulties are the glaring inconsistencies recently discovered between 'old' and 'new' DNS databases [104, 105].

Developing a complete, self-consistent model is more than an academic exercise, because a proper conceptual model of the flow gives researchers the necessary tools to compute high-Reynolds-number practical flows using the Reynolds-averaged Navier–Stokes equations as well as to devise novel flow control strategies and to extend known laboratory-scale control devices to field conditions.

3.4.4. Inner/outer interactions. There is no doubt that significant interactions between the inner and outer layers take place. On energy grounds alone, it is known that in the outer layer the dissipation is larger than the turbulence kinetic energy production [38]. It is therefore necessary for energy to be transported from the inner layer to the outer layer simply to sustain the latter. How that is accomplished and whether coherent structures are the only vehicle to transport energy is not clear, but two distinct schools of thought have emerged. In the first, the large-scale structures dominate and provide the strong buffeting necessary to maintain the low-Reynolds-number turbulence in the viscous region ($y^+ \leq 30$). In the second view, rare, intense wall-events are assigned the active role and, through outward turbulence diffusion, provide the necessary energy supply to maintain the outer region. As mentioned in the previous subsubsection, both views have some loose ends.

Based on a large number of space-time, two-point correlation measurements of u and v, Kovasznay et al. [62] suggested that the outer region of a turbulent boundary layer is dominated by large eddies. The interface between the turbulent flow and the irrotational fluid outside the boundary layer is highly corrugated with a root-mean-square slope in the x–y plane of roughly 0.5. The three-dimensional bulges are elongated in the streamwise direction with an aspect ratio of approximately 2:1, and have a characteristic dimension, in the wall-normal direction, of between 0.5 δ and δ. They appear quasi-periodically and are roughly similar to each other. Kovasznay et al. allowed that the large eddies are passive in the sense that the wall events and not these eddies are responsible for producing the Reynolds stress. Kovasznay [52] advanced the hypothesis that wall bursting starts a chain reaction of some sort at all intermediate scales culminating into a sequence of amalgamations that eventually leads to the large structures. As mentioned earlier, such hierarchical amalgamation of scales has not been directly observed in the laboratory.

Head and Bandyopadhyay [67], on the other hand, suggested that the very existence of the large eddies at high Reynolds numbers is in doubt. Their combined flow visualization/hot-wire probe experiments are unique in that an unusually large range of Reynolds number was investigated, $\Re_\theta = 500$–$17{,}500$, allowing them to clarify unambiguously Reynolds number effects on the structure of the boundary layer. Head and Bandyopadhyay maintained that a large structure seen in typical flow visualization experiments is nothing but the slow overturning of a random collection of smaller-scale hairpin vortices: just a few or even a single isolated vortex loop at low Reynolds numbers (say, $\Re_\theta < 1{,}000$), but a large number of them at high Reynolds numbers (say, $\Re_\theta > 5{,}000$). A brisker rate of rotation of the isolated (fat) vortex loop is observed at the lowest Reynolds number, consistent with prior observations of large eddies in low-speed experiments. The hairpins are inclined at around 45° to the plane of the flow over a major part of the layer thickness. In Head and Bandyopadhyay's view [67], the entire turbulent boundary layer largely consists of vortex loops that become increasingly elongated as the Reynolds number increases. The so-called large eddies, on the other hand, do not appear to exhibit any particular coherent motion beyond a relatively slow overturning or toppling due to shear.

Corroborative evidence for the hairpin angle of inclination of 45° comes from the simultaneous, multiple-point hot-wire measurements of Alving et al. [106] in both a canonical turbulent boundary layer and a boundary layer recovering from the effects of strong convex curvature. Their cross-correlation results are consistent with the observation of large-scale structures spanning the entire shear layer and inclined at angles in the range of 35–45° near the outer edge of the boundary layer, but at continuously decreasing angles as the wall is approached.

A typical large eddy at high Reynolds numbers is consistent with the statistical findings of Brown and Thomas [107], who have shown by using conditional-averaging techniques that a typical large structure in a turbulent boundary layer has an upstream rotational/irrotational interface inclined at 18° to the flow direction. Head and Bandyopadhyay [67] have observed such individual structures only at higher $\Re_\theta$ ($> 5{,}000$). It is possible to arrive precisely at this slope by modeling the large structure to be composed of hairpin vortices formed at regular intervals [108]. Such large structures composed of many hairpin vortices have not been observed in the low-Reynolds-number DNS simulations [73]. Note, however, that newer DNS databases [104, 105] beg to differ.

3.4.5. Regeneration. Robinson [41] summarizes many of the conceptual models advanced by different researchers to explain how a wall-bounded turbulent flow maintains itself. Among those reviewed are the models advocated in References [79, 109–116]. Some of those conceptual models emphasize a particular aspect of the flow dynamics as for example the bursting cycle, while others are more ambitious and attempt to include both the inner and outer structures as well as their interactions. Several viewpoints on the regeneration mechanisms of wall turbulence are represented in the books edited by Kline and Afgan [117] and by Panton [51].

Robinson [116] also lists significant contributions that utilize structural information to predict statistical quantities or invoke a simplified form of the governing equations to model the dynamics of the near-wall turbulence-production process. Among the predictive models are those discussed in References [38, 118–127].

Other, potentially useful, predictive models not discussed by Robinson [41] include those based on stability considerations [128, 129], based on the turbulence energy equation [130], based on the u–v velocity-quadrant statistical description of the organized motions [131], and based on a single hairpin-like vortex in a unit domain of turbulence production [132–134]. These models account explicitly for Reynolds number effects and therefore might be useful for practical Reynolds numbers.

Inevitably in almost all the conceptual models, the omnipresent hairpin vortex (or horseshoe vortex at low $\Re_\theta$) plays a key role. Such a vortex has been proposed earlier by Theodorsen [135, 136] on intuitive grounds as the primary structure responsible for turbulence production and dissipation in the boundary layer. Theodorsen's tornado-like vortices form astride near-wall, low-speed regions of fluid and grow outward with their heads inclined at 45° to the flow direction.

Black [110, 137] conducted a more rigorous analytical work to show the fundamental role of hairpin vortices in the dynamics of wall-bounded flows. His basic premise is that the primary role of the random turbulent motion is not to transfer mean momentum directly but rather to excite strong, three-dimensional instability of the sublayer, which is a powerhouse of vorticity. In Black's model, trains of discrete horseshoes are generated by repetitive, localized nonlinear instabilities within the viscous sublayer. The vortical structures are shed and outwardly migrate from the near-wall region in a characteristic, quasi-frozen spatial array. The horseshoes inviscidly induce an outflow of low-speed fluid from within the vortex loops, creating motions that would be seen by a stationary probe as sharp, intermittent spikes of Reynolds stress. Because of the continuous creation of new vortex loops that replace older elements, the lifetime of the vortical array is much longer than that for its individual members. According to Black [110], such organized structures are responsible for the efficient mass and momentum transfer within a turbulent boundary layer.

Sreenivasan [103] offers a similar model to that of Black [110]. The essential structures of the boundary layer, including the hairpin vortices, result from the instability of a caricature flow in which all the mean flow vorticity has been concentrated into a single fat sheet.

As a parting remark to this subsubsection, it might be instructive to recall that hairpin vortices play an important role also in the laminar-to-turbulence transition of boundary layer flows. Essentially, these hairpins are the result of the nonlinear tertiary instability of the three-dimensional peak/valley pattern, which itself is the secondary instability of the primary Tollmien–Schlichting waves [138].

4. Flow control

4.1. The genesis. The art of flow control probably has its roots in prehistoric times when streamlined spears, sickle-shaped boomerangs, and fin-stabilized arrows evolved empirically [139] by the sheer perseverance of archaic Homo sapiens who knew nothing about air resistance or aerodynamic principles. Three *Aerodynamically correct* wooden spears were excavated two decades ago in an open-pit coal mine near Hanover, Germany [140]. Archeologists dated the carving of those complete spears to about 400,000 years ago [141], which strongly suggests early Stone Age ancestors possessing resourcefulness and skills once thought to be characteristics that came only with fully-modern Homo sapiens.

Modern man also artfully applied flow control methods to achieve certain technological goals. Relatively soon after the dawn of civilization and the establishment of an agriculture way of life 8,000 years ago, complex systems of irrigation were built along inhabited river valleys to control the water flow, thus freeing man from the vagaries of the weather. Some resourceful albeit mischievous citizens of the Roman Empire discovered that adding the right kind of diffuser to the calibrated convergent nozzle ordinarily installed at home outlets of the public water main significantly increased the charge of potable water over that granted by the emperor. For centuries, farmers knew the value of windbreaks to keep top soil in place and to protect fragile crops.

The science of flow control originated with Prandtl [142], who introduced the boundary layer theory, explained the physics of the separation phenomena, and described several experiments in which a boundary layer was controlled. Thus the birth of the scientific method to control a flow field. Slowly but surely, the choice of flow control devices is no longer a trial and error feat, but physical reasoning and even first principles more often than not are used for rational design of such artifacts.

Prandtl [142] used active control of the boundary layer to show the great influence such a control exerted on the flow pattern. He used suction to delay boundary-layer separation from the surface of a cylinder. Notwithstanding Prandtl's success, aircraft designers in the three decades following his convincing demonstration were accepting lift and drag of airfoils as predestined characteristics with which no man could or should tamper [143]. This predicament changed mostly due to the German research in boundary-layer control pursued vigorously shortly before and during the Second World War. In the two decades following that war, extensive research on laminar flow control, where the boundary layer formed along an aircraft's wing is kept in the low-drag laminar state, was conducted in Europe and the United States, culminating in the successful flight test program of the X-21 where suction was used to delay transition on a swept wing up to a chord Reynolds number of 4.7×10^7. The oil crisis of the early 1970s brought renewed interest in novel methods of flow control to reduce skin-friction drag even in turbulent boundary layers. In the 1990s, the need to reduce the emissions of greenhouse gases and to construct supermaneuverable fighter planes, faster/quieter underwater vehicles, and hypersonic transport aircraft (e.g., the U.S. National Aerospace Plane) provided new challenges for researchers in the field of flow control.

4.2. Interrelation. A particular control strategy is chosen based on the kind of flow and the control goal to be achieved. Flow control goals are strongly, often adversely, interrelated; and there lies the challenge of making the tough compromises. There are several different ways for classifying control strategies to achieve a desired effect. Presence or lack of walls,

Reynolds and Mach numbers, and the character of the flow instabilities are all important considerations for the type of control to be applied. All these seemingly disparate issues are what place the field of flow control in a unified framework, as exhaustively covered in the book by Gad-el-Hak [102].

What does the engineer want to achieve when attempting to manipulate a particular flow field? Typically he or she aims at reducing the drag, enhancing the lift, augmenting the mixing of mass, momentum, or energy, suppressing the flow-induced noise, or a combination thereof. To achieve any of these useful end results, for either free-shear or wall-bounded flows, transition from laminar to turbulent flow may have to be either delayed or advanced, flow separation may have to be either prevented or provoked, and finally turbulence levels may have to be either suppressed or enhanced. All those engineering goals and the corresponding flow changes intended to effect them are schematically depicted in Fig. 8. None of that is particularly difficult if taken in isolation, but the challenge is in achieving a goal using a simple device, inexpensive to build as well as to operate, and, most importantly, has minimum 'side effects'. For this last hurdle, the interrelation between control goals must be elaborated, and this is what is attempted below, using, as an example, boundary-layer flows.

An external wall-bounded flow, such as that developing on the exterior surface of a wing, can be manipulated to achieve transition delay, separation postponement, lift increase, skin-friction and pressure-drag reduction, turbulence augmentation, mixing enhancement, and noise suppression. These objectives are interrelated and are not necessarily mutually exclusive, as indicated schematically in Fig. 9. If the boundary layer around the wing becomes turbulent, its resistance to separation is enhanced and more lift can be obtained at increased incidence. On the other hand, the skin-friction drag for a laminar boundary

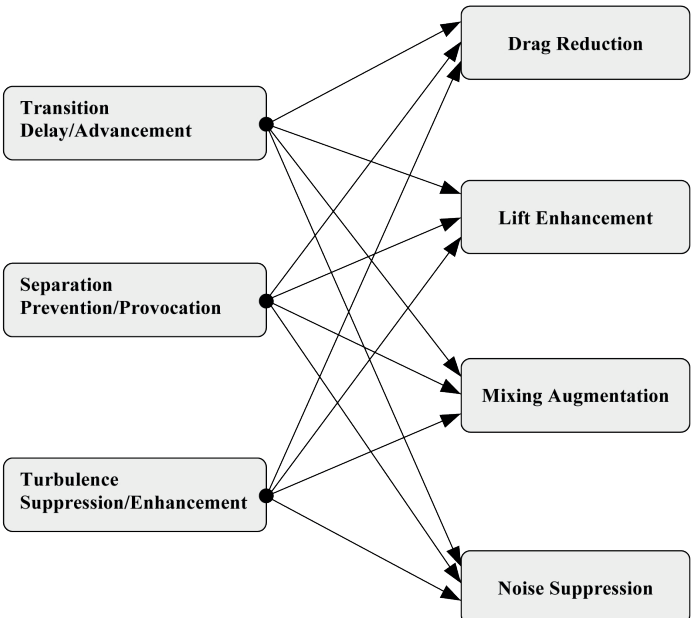

Fig. 8. Engineering goals and corresponding flow changes. Block diagram adapted from Gad-el-Hak [102]

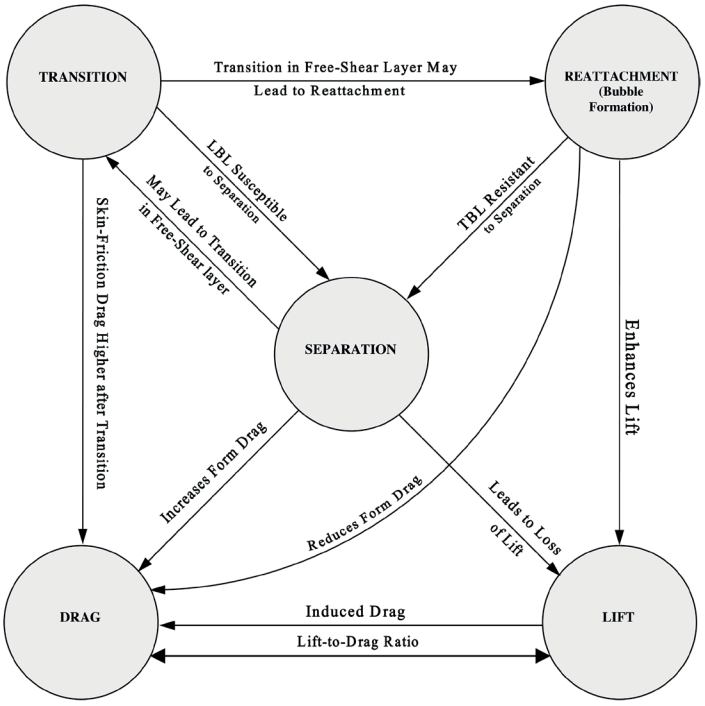

Fig. 9. Partial representation of the interrelation among flow control goals. Block diagram adapted from Gad-el-Hak [102]

layer can be as much as an order of magnitude less than that for a turbulent one. If transition is delayed, lower skin friction and lower flow-induced noise are achieved. However, a laminar boundary layer can support only very small adverse pressure gradients without separation. At the slightest increase in angle of attack or some other provocation, such boundary layer detaches from the wing's surface and subsequent loss of lift and increase in form drag occur. Once the laminar boundary layer separates, a free-shear layer forms, and for moderate Reynolds numbers transition to turbulence takes place. Increased entrainment of high-speed fluid due to the turbulent mixing may result in reattachment of the separated region and formation of a laminar separation bubble. At higher incidence, the bubble breaks down, either separating completely or forming a longer bubble. In either case, the form drag increases and the lift curve's slope decreases. The ultimate goal of all this is to improve the airfoil's performance by increasing the lift-to-drag ratio. However, induced drag is caused by the lift generated on a wing with a finite span. Moreover, more lift is generated at higher incidence, but form drag also increases at these angles.

All of the above points to potential conflicts as one attempts to achieve a particular control goal only to affect adversely another goal. An ideal method of control that is simple, inexpensive to build and operate, and does not have any tradeoffs does not exist, and the skilled engineer has to make continuous compromises to achieve a particular design goal.

Flow control is most effective when applied near the transition or separation points, which are critical flow regimes where flow instabilities magnify quickly. Therefore, delaying or advancing the laminar-to-turbulence transition and preventing

or provoking separation are relatively easier to accomplish. Reducing the skin-friction drag in a non-separating turbulent boundary layer, where the flow is not critical and the mean flow is quite stable, is a more challenging problem. Yet, even a modest reduction in the fluid resistance to the motion of, for example, the worldwide commercial airplane fleet is translated into annual fuel savings estimated to be in the billions of dollars. Newer ideas for turbulent flow control focus on targeting coherent structures, which are quasi-periodic, organized, large-scale vortex motions embedded in a random, or incoherent, flow field (Figs 4–6).

4.3. Future systems. Future systems for control of turbulent flows in general and turbulent boundary layers in particular could greatly benefit from the merging of the science of chaos control, the technology of microfabrication, and the newest computational tools collectively termed soft computing. Control of chaotic, nonlinear dynamical systems has been demonstrated theoretically as well as experimentally, even for multi-degree-of-freedom systems. Microfabrication is an emerging technology that has the potential for mass-producing inexpensive, programmable sensor-actuator chips, where each sensor or actuator is as small as a few micrometers. Soft-computing tools include neural networks, fuzzy logic, and genetic algorithms. They have advanced and become more widely used in the last few decades, and could be very useful in constructing effective adaptive controllers. Such futuristic systems are envisaged as consisting of a colossal number of intelligent, interactive, microfabricated wall sensors and actuators arranged in a checkerboard pattern and targeted toward specific organized structures that occur quasi-randomly (or quasi-periodically) within a turbulent flow. Sensors would detect oncoming coherent structures, and adaptive controllers would process the sensors' information and provide control signals to the actuators, which in turn would attempt to favorably modulate the quasi-periodic events. A finite number of wall sensors perceives only partial information about the flow field. However, a low-dimensional dynamical model of the near-wall region used in a Kalman filter can make the most of this partial information. Conceptually all of that is not too difficult, but in practice the complexity of such control systems is daunting and much research and development work remains.

4.4. Control strategies. Different levels of "intelligence" can be imbued into a particular control system (Fig. 10). The control can be passive, requiring no auxiliary power and no control loop, or active, requiring energy expenditure. There are numerous passive control strategies, but we cite here just three examples: (i) streamlining an airfoil to delay transition, delay separation, and achieve maximum lift-to-drag ratio [144, 145]; compliant coatings [146, 147]; and (iii) tuned subsurface phonons [148, 149].

Active control requires a control loop and is further divided into predetermined or reactive. Predetermined active control includes the application of steady or unsteady energy input without regard to the particular state of the system—for example, a pilot engaging the wing's flaps for takeoff. The control loop in this case is open, as shown in Fig. 11a, and no

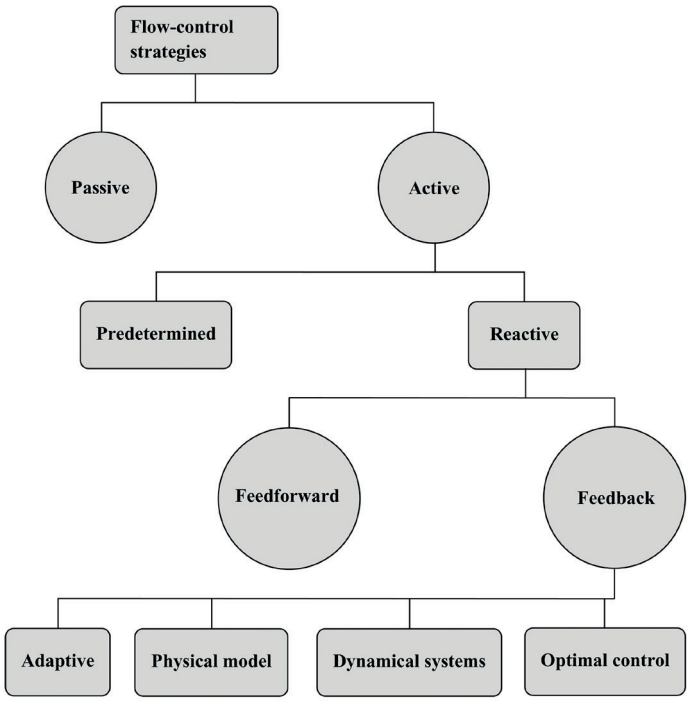

Fig. 10. Classification of control strategies. Block diagram adapted from Gad-el-Hak [102]

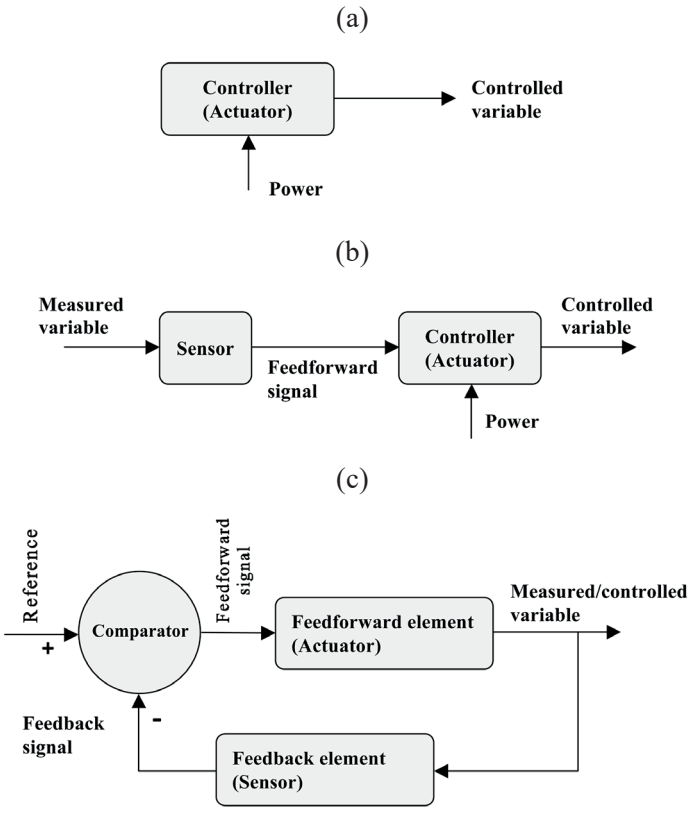

Fig. 11. Different control loops for active flow control. a) Predetermined, open-loop control; b) Reactive, feedforward, open-loop control; c) Reactive, feedback, closed-loop control. Block diagram adapted from Gad-el-Hak [102]

sensors are required. Because no sensed information is being fed forward, this open control loop is not a feedforward one. This subtle point is often confused in the literature, blurring predetermined control with reactive, feedforward control [150].

Reactive, or 'smart', control is a special class of active control where the control input is continuously adjusted based on measurements of some kind. The control loop in this case can be an open, feedforward one (Fig. 11b), or a closed, feedback loop (Fig. 11c). Achieving that level of autonomous control (that is without human interference) is the ultimate goal of 'smart-wing' designers. In feedforward control, the measured variable and the controlled variable are not necessarily the same. For example, the pressure can be sensed at an upstream location, and the resulting signal is used together with an appropriate control law to actuate a shape change that in turn influences the shear stress (that is skin friction) at a downstream position. Feedback control, on the other hand, necessitates that the controlled variable be measured, fed back, and compared with a reference input. Reactive, feedback control is further classified into four categories: (i) adaptive; (ii) physical model-based; (iii) dynamical systems-based; and (iv) optimal control. We will return to this point in Section 5. An example of reactive control is the use of distributed sensors and actuators on a wing's surface to detect certain coherent flow structures and, based on a sophisticated control law, subtly morph the wing to suppress those structures in order to dramatically reduce the skin-friction drag.

4.5. Reactive control.

4.5.1. Introductory remarks. That a turbulent flow is difficult to control is an understatement. This of course applies to man-made systems; bald eagles, for example, effortlessly perform exquisite turbulence control seemingly without any knowledge of fluid Mechanics.

Aside from the fact that a non-separating turbulent flow is not a critical flow regime, and hence requiring strong input to perturb, the governing equations are nonlinear and have no known analytical solution to provide the time-dependent, three-dimensional, stochastic flow field. The tradeoff/penalty for passive or predetermined active control often exceeds the benefit. Reactive control, on the other hand, is both complex and difficult to accomplish mostly because an optimum control plant needs the all-illusive analytical solution to the first-principles dynamical equations. The computer-intensive direct numerical solutions to the instantaneous equations are too slow to be of much use in predicting what happens next, a necessary step for rational reactive control. The operator of the control plant is then forced to rely on heuristic methods, or at best on suboptimal control [151].

Targeted control implies sensing and reacting to a particular quasi-periodic structure in the boundary layer. The wall seems to be the logical place for such reactive control, because of the relative ease of placing something in there, the sensitivity of the flow in general to surface perturbations, and the proximity and therefore accessibility to the dynamically all important near-wall coherent events. According to Wilkinson [152], there are very few actual experiments that use embedded wall sensors to initiate a surface actuator response [153–156]. That thirty-year-old assessment is fast changing, however, with the introduction of microfabrication technology that has the potential for producing small, inexpensive, programmable sensor/actuator chips. Witness the more recent reactive control attempts by Kwong and Dowling [157], Reynolds [158], Jacobs et al. [159], Jacobson and Reynolds [160–164], Fan et al. [165], James et al. [166], and Keefe [167]. Fan et al. and Jacobson & Reynolds even considered the use of self-learning neural networks for increased computational speed and efficiency. Relatively recent reviews of reactive flow control include those by Mehregany [172], Gad-el-Hak [168, 169], Lumley [170], McMichael [171], and Ho and Tai [173].

Numerous methods of flow control have already been successfully implemented in practical engineering devices. Yet, limitations exist for some familiar control techniques when applied to specific situations. For example, in attempting to reduce the drag or enhance the lift of a body having a turbulent boundary layer using global suction, global heating/cooling, or global application of electromagnetic body forces, the actuators' energy expenditure often exceeds the saving derived from the predetermined active control strategy. What is needed is a way to reduce this penalty to achieve a more efficient control. Reactive control geared specifically toward manipulating the coherent structures in turbulent shear flows, though considerably more complicated than passive control or even predetermined active control, has the potential to do just that. As will be argued in the following subsubsection as well as in Section 5, future systems for control of turbulent flows in general and turbulent boundary layers in particular could greatly benefit from the merging of the science of chaos control, the technology of microfabrication, and the newest computational tools collectively termed soft computing. Such systems are envisaged as consisting of a large number of intelligent, communicative wall sensors and actuators arranged in a checkerboard pattern and targeted toward controlling certain quasi-periodic, dynamically-significant coherent structures present in the near-wall region.

4.5.2. Targeted control. Successful techniques to reduce the skin friction in a turbulent flow, such as polymers, particles, or riblets, appear to act indirectly through local interaction with discrete turbulent structures–particularly small-scale eddies–within the flow. Common characteristics of all these methods are increased losses in the near-wall region, thickening of the buffer layer, and lowered production of Reynolds shear stress [174]. Methods that act directly on the mean flow, such as suction or lowering of near-wall viscosity, also lead to inhibition of Reynolds stress. However, skin friction is increased when any of these velocity-profile modifiers is applied globally [102]. A few exceptions exists. For example, George Em Karniadakis and his colleagues [175] achieved—at least numerically—70% skin-friction reduction by the action of a localized steady force acting in the near-wall region of a channel flow. In a physical experiment, Li & Zhou [176] realized comparable drag reduction using periodic blowing through an array of streamwise slits.

Back to control strategies that act directly on the mean flow, could these seemingly inefficient techniques, e.g. global

suction, be used more sparingly and be optimized to reduce their associated penalty? It appears that the more successful drag-reducing methods, e.g. polymers, act selectively on particular scales of motion and are thought to be associated with stabilization of the secondary instabilities. It is also clear that energy is wasted when suction or heating/cooling is used to suppress the turbulence throughout the boundary layer, whilst the main interest is to affect a near-wall phenomenon. One ponders, what would become of wall turbulence if specific coherent structures were to be targeted, via a reactive control scheme, for modification?

The myriad of organized structures present in all shear flows is instantaneously identifiable, quasi-periodic motions [39, 41]. Bursting events in wall-bounded flows, for example, are both intermittent and random in space as well as time. The random aspects of these events reduce the effectiveness of a predetermined active control strategy. If such structures are detected and altered, on the other hand, net performance gain might be achieved. It seems clear, however, that temporal phasing as well as spatial selectivity would be required to achieve proper control targeted toward random events.

A nonreactive version of the above idea is the selective suction technique, which combines suction to achieve an asymptotic turbulent boundary layer and longitudinal riblets to fix the location of low-speed streaks. Although far from indicating net drag reduction, the available results are encouraging and further optimization is needed. When implemented via an array of reactive control loops, the selective suction method is potentially capable of skin-friction reduction that approaches 60%.

The papers by Gad-el-Hak and Blackwelder [177, 178] and the patent by Blackwelder and Gad-el-Hak [179] mark the genesis of the selective suction concept. These researchers suggested that one possible means of minimizing the suction rate is to identify where a low-speed streak is presently located and then apply a minute amount of suction under it. Assuming that the production of turbulence kinetic energy is due to the instability of an inflectional $U(y)$ velocity profile, one needs to remove only enough fluid so that the inflectional nature of the profile is alleviated. An alternative technique that could conceivably reduce the Reynolds stress is to inject fluid selectively under the high-speed regions. The immediate effect of normal injection would be to decrease the viscous shear at the wall resulting in less drag. In addition, the velocity profiles in the spanwise direction, $U(z)$, would have a smaller shear, $\partial U/\partial z$, because the suction/injection would create a more uniform flow.

Since Swearingen and Blackwelder [88, 180] have found that inflectional $U(z)$ profiles occur as often as inflection points are observed in $U(y)$ profiles, suction under the low-speed streaks and injection under the high-speed regions would decrease this shear and hence the resulting instability. The combination of selective suction and injection is sketched in Fig. 12. In Fig. 12a, the streamwise vortices are idealized by a periodic distribution in the spanwise direction. The dashed lines in Figs 12b and 12c respectively show the instantaneous velocity profiles without transpiration at constant y and z locations. Clearly, the $U(z)$ profile is inflectional, having two inflection points per

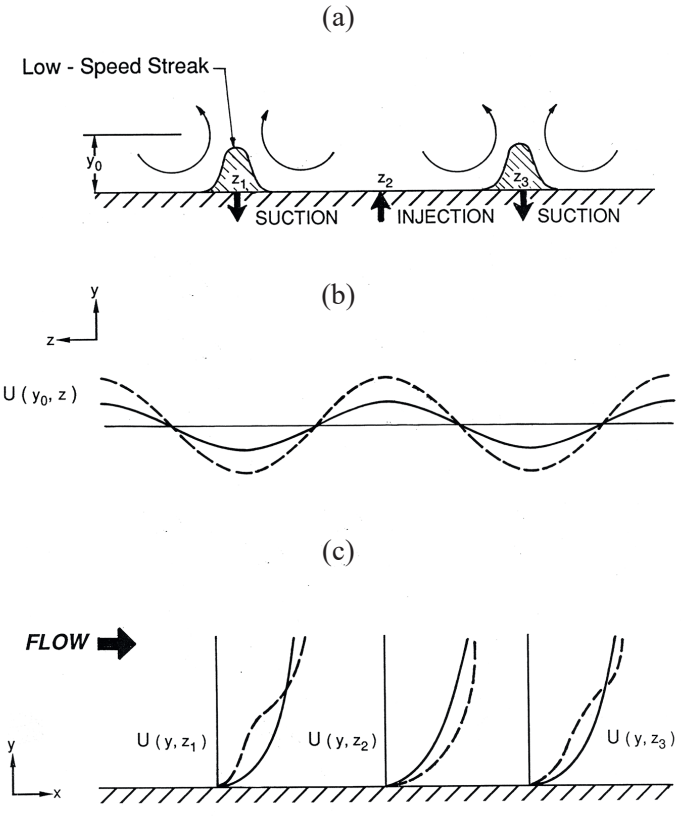

Fig. 12. Effect of suction/injection on velocity profiles. Broken lines: reference profiles; solid lines: profiles with transpiration applied. a) Streamwise vortices in the y-z plane, suction/injection applied at z_1, z_2, and z_3. b) Resulting spanwise velocity distribution at $y = y_0$. c) Velocity profiles normal to the surface. From Gad-el-Hak & Blackwelder [178]

wavelength. At z_1 and z_3, an inflectional $U(y)$ profile is also evident. The solid lines show the same profiles with suction at z_1 and z_3 and injection at z_2. In all cases, the shear associated with the inflection points would have been reduced. Since the inflectional profiles are all inviscidly unstable with growth rates proportional to the shear, the suction/injection process would weaken the resulting instabilities.

Gad-el-Hak and Blackwelder [178] demonstrated the feasibility of the selective suction as a drag-reducing concept. Following the method proposed by Gad-el-Hak and Hussain [99], low-speed streaks were artificially generated in a laminar boundary layer using three spanwise suction holes, and a hot-film probe was used to record the near-wall signature of the streaks. An open, feedforward control loop with a phase lag was used to activate a predetermined suction from a longitudinal slot located in between the spanwise holes and the downstream hot-film probe. An equivalent suction coefficient of $C_q = 0.0006$ was sufficient to eliminate the artificial events and prevent bursting. This rate is five times smaller than the asymptotic suction coefficient for a corresponding turbulent boundary layer. If this result were sustained in a naturally developing turbulent boundary layer, a skin-friction reduction of close to

60% would be attained. Gad-el-Hak and Blackwelder [178] proposed to combine suction with non-planar surface modifications. Minute longitudinal roughness elements if properly spaced in the spanwise direction greatly reduce the spatial randomness of the low-speed streaks [181]. By withdrawing the streaks forming near the peaks of the roughness elements, less suction should be required to achieve an asymptotic boundary layer. Experiments by Wilkinson and Lazos [182, 183] combine suction/blowing with thin-element riblets. Although no net drag reduction is yet attained in these experiments, their results indicate some advantage of combining suction with riblets as proposed by Gad-el-Hak and Blackwelder [177, 178].

The numerical experiments of Choi et al. [184] also validate the concept of targeting suction/injection to specific near-wall events in a turbulent channel flow. Based on complete interior flow information and using the rather simple heuristic control law proposed earlier by Gad-el-Hak and Blackwelder [177], Choi et al.'s direct numerical simulations indicate a 20% net drag reduction accompanied by significant suppression of the near-wall structures and the Reynolds stress throughout the entire wall-bounded flow. When only wall information was used, a drag reduction of 6% was observed; a rather disappointing result considering that sensing and actuation took place at every grid point along the computational wall. In a practical implementation of this technique, even fewer wall sensors would perhaps be available, measuring only a small subset of the accessible information and thus requiring even more sophisticated control algorithms to achieve the same degree of success. Low-dimensional models of the near-wall flow and soft-computing tools can help in constructing more effective control algorithms.

Time sequences of the numerical flow field of Choi et al. [184] indicate the presence of two distinct drag-reducing mechanisms when selective suction/injection is used: first, deterring the sweep motion—without modifying the primary streamwise vortices above the wall—and consequently moving the high-shear regions from the surface to the interior of the channel, thus directly reducing the skin friction; and second, changing the evolution of the wall vorticity layer by stabilizing and preventing the lifting of near-wall spanwise vorticity, thus suppressing a potential source of new streamwise vortices above the surface and interrupting a seemingly important regeneration mechanism of turbulence.

Three modern developments have relevance to the issue at hand. Firstly, the recently demonstrated ability to revert a chaotic system to a periodic one may provide optimal nonlinear control strategies for further reduction in the amount of suction (or the energy expenditure of any other active wall-modulation technique) needed to attain a given degree of flow stabilization. This is important since net drag reduction achieved in a turbulent boundary layer increases as the suction coefficient decreases. Secondly, to selectively remove the randomly occurring low-speed streaks, for example, would ultimately require reactive control. In that case, an event is targeted, sensed, and subsequently modulated. Microfabrication technology provides opportunities for practical implementation of the required large array of inexpensive, programmable sensor/actuator chips. Thirdly, newly introduced soft-computing tools include neural networks, fuzzy logic, and genetic algorithms. Those are now more advanced as well as more widely used as compared to just few years ago. Soft-computing tools could be very useful in constructing effective adaptive controllers. All three novel developments will be discussed in the next section.

5. Flow control and coherent structures: association

Reactive control goes by different names: selective, targeted, opposition, smart, feedback/feedforward control, and closed- or open-loop control. It is a form of control that requires energy expenditure, but the primary goal is to achieve sufficient benefit to justify the energy expenditure. The main thesis of this article is to advocate the type of 'smart' control that target specific coherent structures for modification, in contrast to brute-force control of the entire flow field. In this section, we elaborate on the association between reactive control and coherent structures.

5.1. Reactive feedback control. As was schematically depicted in Fig. 10, a control device can be passive, requiring no auxiliary power, or active, requiring energy expenditure. Active control is further divided into predetermined or reactive. Predetermined control includes the application of steady or unsteady, spatially homogeneous or inhomogeneous, energy input without regard to the particular state of the flow. The control loop in this case is open as was shown in Fig. 11a, and no sensors are required. Because no sensed information is being fed forward, this open control loop is not a feedforward one. Reactive control is a special class of active control where the control input is continuously adjusted based on measurements of some kind. The control loop in this case can either be an open, feedforward one (Fig. 11b) or a closed, feedback loop (Fig. 11c).

The distinction between feedforward and feedback is particularly important when dealing with the control of flow structures that convect over stationary sensors and actuators. In feedforward control, the measured variable and the controlled variable may differ. For example, the pressure or velocity can be sensed at an upstream location, and the resulting signal is used together with an appropriate control law to trigger an actuator that in turn influences the velocity at a downstream position. Feedback control, on the other hand, necessitates that the controlled variable be measured, fed back, and compared with a reference input.

Moin and Bewley [185] categorized reactive feedback control strategies by examining the extent to which they are based on the governing flow equations. Four categories are discerned (Fig. 10): (i) adaptive; (ii) physical model-based; (iii) dynamical systems-based; and (iv) optimal control. Note that except for adaptive control, the other three categories of reactive feedback control can also be used in the feedforward mode or the combined feedforward–feedback mode. Also, in a convective environment such as that for a boundary layer, a controller would perhaps combine feedforward and feedback information and may include elements from each of the four classifications. Each of the four categories is briefly described below.

Adaptive schemes attempt to develop models and controllers via some learning algorithm without regard to the details of the flow physics. System identification is performed independently of the flow dynamics or the Navier–Stokes equations that govern this dynamics. An adaptive controller tries to optimize a specified performance index by providing a control signal to an actuator. In order to update its parameters, the controller thus requires feedback information relating to the effects of its control. The most recent innovation in adaptive flow control schemes involves the use of neural networks that relate the sensor outputs to the actuator inputs through functions with variable coefficients and nonlinear, sigmoid saturation functions. The coefficients are updated using the so-called back-propagation algorithm, and complex control laws can be represented with a sufficient number of terms. Manual tuning is required, however, to achieve good convergence properties. Fan et al. [165] and Jacobson and Reynolds [161, 163, 164] have used, with different degrees of success, the nonlinear adaptive technique to control, respectively, the transition process and the bursting events in turbulent boundary layers.

Heuristic physical arguments can instead be used to establish effective control laws. That approach obviously will work only in situations in which the dominant physics are well understood. An example of this strategy is the active cancellation scheme, used by Gad-el-Hak and Blackwelder [178] in a physical experiment and by Choi et al. [184] in a numerical experiment, to reduce the drag by mitigating the effect of near-wall vortices. As mentioned earlier, the idea is to oppose the near-wall motion of the fluid, caused by the streamwise vortices, with an opposing wall control, thus lifting the high-shear region away from the surface and interrupting the turbulence regeneration mechanism.

Nonlinear dynamical systems theory allows turbulence to be decomposed into a small number of representative modes whose dynamics are examined to determine the best control law. The task is to stabilize the attractors of a low-dimensional approximation of a turbulent chaotic system. The best-known strategy is the OGY's method (to be discussed in Subsection 5.3). When applied to simpler, small-number of degrees of freedom systems, the method achieves stabilization with minute expenditure of energy. This and other chaos control strategies, especially as applied to the more complex turbulent flows, will be revisited later.

Finally, optimal control theory applied directly to the Navier–Stokes equations can, in principle, be used to minimize a cost function in the space of the control. This strategy provides perhaps the most rigorous theoretical framework for flow control. As compared to other reactive control strategies, optimal control applied to the full Navier–Stokes equations is also the most computer-time intensive. In this method, feedback control laws are systematically derived for the most efficient distribution of control effort to achieve a desired goal. Abergel and Temam [186] developed such optimal control theory for suppressing turbulence in a numerically simulated, two-dimensional Navier–Stokes flow, but their method requires impractical full flow-field information. Choi et al. [187] developed a more practical, wall-information-only, sub-optimal control strategy that they applied to the one-dimensional stochastic Burgers equation. Moin and his colleagues [185, 188, 189] later extended the sub-optimal control theory to a numerically simulated turbulent channel flow. The book edited by Sritharan [190] provides eight articles that focus on the mathematical aspects of optimal control of viscous flows.

5.2. Required characteristics. The randomness of the bursting events necessitates temporal phasing as well as spatial selectivity to effect selective control. Practical applications of methods targeted at controlling a particular turbulent structure to achieve a prescribed goal would therefore require implementing a large number of surface sensors/actuators together with appropriate control algorithms. That strategy for controlling wall-bounded turbulent flows has been advocated by, among others and in chronological order, Gad-el-Hak and Blackwelder [177, 178], Lumley [191, 192], Choi et al. [193], Mehregany [172], Reynolds [158], Jacobson and Reynolds [161, 163], Moin and Bewley [185], Gad-el-Hak [168, 169, 194], McMichael [171], Blackwelder [58], Delville et al. [42], and Perrier [195].

It is instructive to estimate some representative characteristics of the required array of sensors/actuators. Consider a typical commercial aircraft cruising at a speed of $U_\infty = 300$ m/s, at an altitude of 10 km. The density and kinematic viscosity of air and the unit Reynolds number in this case are, respectively, $\rho = 0.4$ kg/m^3, $\nu = 3\times10^{-5}$ m^2/s, and $Re = 10^7$/m. Assume further that the portion of fuselage to be controlled has a turbulent boundary layer which characteristics are identical to those for a zero-pressure-gradient flat plate at a distance of 1 m from the leading edge. In this case, the skin-friction coefficient and the friction velocity are, respectively, $C_f = 0.003$ and $u_\tau = 11.62$ m/s. At this location, one viscous wall unit is only $\nu/u_\tau = 2.6$ μm. In order for the surface array of sensors/actuators to be hydraulically smooth, it should not protrude beyond the viscous sublayer, or $5\nu/u_\tau = 13$ μm. Low-speed streaks are the most visible, reliable, and detectable indicators of the pre-burst turbulence production process. The detection criterion is simply low velocity near the wall, and the actuator response should be to accelerate (or to remove) the low-speed region before it breaks down. Local wall motion, tangential injection, suction, cooling, or electromagnetic body force, all triggered on sensed wall-pressure or wall-shear stress, could be used to cause local acceleration of the near-wall fluid.

The numerical experiments of Berkooz et al. [196] indicate that effective control of a bursting pair of rolls may be achieved by using the equivalent of two wall-mounted shear sensors. If the goal is to stabilize or to eliminate all low-speed streaks in the boundary layer, a reasonable estimate for the spanwise and streamwise distances between individual elements of a checkerboard array are, respectively, 100 and 1,000 wall units, or 260 μm and 2,600 μm, for our particular example. A reasonable size for each element is probably one-tenth of the spanwise separation, or 26 μm. A (1 m$\times$1 m) portion of the surface would have to be covered with about $n = 1.5$ million elements. This is a colossal number, but the density of sensors/actuators could be considerably reduced if we moderate our goal of targeting

every single bursting event (and also if less conservative assumptions are used).

It is well known that not every low-speed streak leads to a burst. On the average, a particular sensor would detect an incipient bursting event every wall-unit interval of $P^+ = Pu_\tau^2/\nu = 250$, or $P = 56$ μs. The corresponding dimensionless and dimensional frequencies are, respectively, $f^+ = 0.004$ and $f = 18$ kHz. At different distances from the leading edge and in the presence of nonzero pressure gradient, the sensors/actuators array would have different characteristics, but the corresponding numbers would still be in the same ballpark as estimated in here.

As a second example, consider an underwater vehicle moving at a speed of $U_\infty = 10$ m/s. Despite the relatively low speed, the unit Reynolds number is still the same as estimated above for the air case, $Re = 10^7$/m, due to the much lower kinematic viscosity of water. At 1 m from the leading edge of an imaginary flat plate towed in water at the same speed, the friction velocity is only $u_\tau = 0.39$ m/s, but the wall unit is still the same as in the aircraft example, $\nu/u_\tau = 2.6$ μm. The density of required sensors/actuators array is the same as computed for the aircraft example, $n = 1.5\times10^6$ elements/m^2. The anticipated average frequency of sensing a bursting event is, however, much lower at $f = 600$ Hz.

Similar calculations have been made by Gad-el-Hak [168, 194, 197], Reynolds [158], and Wadsworth et al. [198]. Their results agree closely with the estimates made here for typical field requirements. In either the airplane or the submarine case, the actuator's response need not be too large. Wall displacement on the order of 10 wall units (26 μm in both examples), suction coefficient of about 0.0006, or surface cooling/heating on the order of 40°C/2°C (in the first/second example, respectively) should be sufficient to stabilize the turbulent flow.

As computed in the two examples above, both the required size for a sensor/actuator element and the average frequency at which an element would be activated are within the presently known capabilities of microfabrication technology. The number of elements needed per unit area is, however, alarmingly large. The unit cost of manufacturing a programmable sensor/actuator element would have to come down dramatically, perhaps matching the unit cost of a conventional transistor, before the idea advocated herein would become practical.

The good news is that both examples present "worst possible scenario". First, not every burst or streak has to be eliminated. Second, adverse-pressure-gradient regions are critical flow regimes, which require much smaller number of sensors and actuators, as well as much less energy consumption. And third, on newly envisioned aircraft with blended lift-generating wing body (https://en.wikipedia.org/wiki/Blended_wing_body), a good portion of the wing body is in a transitional state, again a critical flow regime. For those three reasons, a reduction in the required number of sensors/actuators by at least an order of magnitude is readily realizable.

An additional consideration to the size, amplitude, and frequency response is the energy consumed by each sensor/actuator element. Total energy consumption by the entire control system obviously has to be low enough to achieve net savings. Consider the following calculations for the aircraft example. One meter from the leading edge, the skin-friction drag to be reduced is approximately 54 N/m^2. Engine power needed to overcome this retarding force per unit area is 16 kW/m^2, or 10^4 μW/sensor. If a 60% drag-reduction is achieved, this energy consumption is reduced to 4,320 μW/sensor. This number will increase by the amount of energy consumption of a sensor/actuator unit, but hopefully not back to the uncontrolled levels. The voltage across a sensor is typically in the range of $V = 0.1$–1 V, and its resistance is in the range of $R = 0.1$–1 MΩ. This means power consumption by a typical sensor in the range of $\mathscr{P} = V^2/R = 0.1$–10 μW, well below the anticipated power savings due to reduced drag.

For a single actuator in the form of a spring-loaded diaphragm with a spring constant of $k = 100$ N/m oscillating up and down at the bursting frequency of $f = 18$ kHz with amplitude of $y = 26$ μm, the power consumption is $\mathscr{P} = (1/2)ky^2f = 600$ μW/actuator. If suction is used instead, $C_q = 0.0006$, and assuming a pressure difference of $\Delta p = 10^4$ N/m^2 across the suction holes/slots, the corresponding power consumption for a single actuator is $\mathscr{P} = C_qU_\infty\Delta p/\mathrm{n} = 1{,}200$ μW/actuator. It is clear then that when the power penalty for the sensor/actuator is added to the lower-level drag, a net saving is still achievable. The corresponding actuator power penalties for the submarine example are even smaller ($\mathscr{P} = 20$ μW/actuator for the wall motion actuator, and $\mathscr{P} = 40$ μW/actuator for the suction actuator), and larger savings are therefore possible.

5.3. Chaos control.

5.3.1. Nonlinear dynamical systems theory. In the theory of dynamical systems, the so-called butterfly effect denotes sensitive dependence of nonlinear differential equations on initial conditions, with phase-space solutions initially very close together but eventually exponentially separating. The solution of nonlinear dynamical systems of three or more degrees of freedom may be in the form of a strange attractor whose intrinsic structure contains a well-defined mechanism to produce a chaotic behavior without necessarily requiring random forcing. Chaotic behavior is complex, aperiodic, and, though deterministic, appears to be random.

A question arises naturally: just as small disturbances can radically grow within a deterministic system to yield rich, unpredictable behavior, could minute adjustments to a system parameter be used to reverse the process and control, i.e. regularize, the behavior of a chaotic system? That question was answered in the affirmative theoretically as well as experimentally, at least for system orbits that reside on low-dimensional strange attractors [199]. Before describing such strategies for controlling chaotic systems, we first summarize the recent attempts to construct a low-dimensional dynamical systems representation of turbulent boundary layers. Such construction is a necessary first step to be able to use chaos control strategies for turbulent flows. Additionally, as argued by Lumley [170], a low-dimensional dynamical model of the near-wall region used in a Kalman filter [200–202] can make the most of the partial information assembled from a finite number of wall sensors. Such filter minimizes in a least square sense the errors

caused by incomplete information, and thus globally optimizes the performance of the control system.

Boundary layer turbulence is described by a set of nonlinear partial differential equations and is characterized by an infinite number of degrees of freedom. This makes it rather difficult to model the turbulence using a dynamical systems approximation. The notion that a complex, infinite-dimensional flow can be decomposed into several low-dimensional subunits is, however, a natural consequence of the realization that quasi-periodic coherent structures dominate the dynamics of seemingly random turbulent shear flows. This implies that low-dimensional, localized dynamics can exist in formally infinite-dimensional extended systems, such as open turbulent flows. Reducing the flow physics to finite-dimensional dynamical systems enables a study of its behavior through an examination of the fixed points and the topology of their stable and unstable manifolds.

From the dynamical systems theory viewpoint, the meandering of low-speed streaks is interpreted as hovering of the flow state near an unstable fixed point in the low-dimensional state space. An intermittent event that produces high wall stress—e.g., a burst—is interpreted as a jump along a heteroclinic cycle to different unstable fixed point that occurs when the state has wandered too far from the first unstable fixed point. Delaying this jump by holding the system near the first fixed point should lead to lower momentum transport in the wall region and, therefore, to lower skin-friction drag. Reactive control means sensing the current local state and through appropriate manipulation keeping the state close to a given unstable fixed point, thereby preventing further production of turbulence. Reducing the bursting frequency by say 50% may lead to a comparable reduction in skin-friction drag. For a jet, relaminarization may lead to a quiet flow and very significant noise reduction.

In one significant attempt, the proper orthogonal, or Karhunen-Loève, decomposition method has been used to extract a low-dimensional dynamical system from experimental data of the wall region [125, 203]. The articles expressed the instantaneous velocity field of a turbulent boundary layer in terms of experimentally determined eigenfunctions that are in the form of streamwise rolls. Aubry and colleagues expanded the Navier–Stokes equations using those optimally chosen, divergence-free, orthogonal functions, applied a Galerkin projection, and then truncated the infinite-dimensional representation to obtain a ten-dimensional set of ordinary differential equations. These equations represent the dynamical behavior of the rolls, and are shown to exhibit a chaotic regime as well as intermittency due to a burst-like phenomenon. However, Aubry et al.'s ten-mode dynamical system [125] displays a regular intermittency, in contrast both to that in actual turbulence as well as to the chaotic intermittency encountered by Pomeau and Manneville [204] in which event durations are distributed stochastically. Nevertheless, the major conclusion of Aubry et al.'s study is that the bursts appear to be produced autonomously by the wall region even without turbulence, but are triggered by turbulent pressure signals from the outer layer. In a later research by the same group, Berkooz et al. [127] generalized the class of wall-layer models developed by Aubry et al. [125] to permit uncoupled evolution of streamwise and cross-stream disturbances. Berkooz et al.'s results suggest that the intermittent events observed in Aubry et al.'s representation do not arise solely because of the effective closure assumption incorporated, but are rather rooted deeper in the dynamical phenomena of the wall region. The book by Holmes et al. [33] details the Cornell research group attempts at describing turbulence as a low-dimensional dynamical system.

Bernd Noack has been quite prolific during the past few years in advancing the idea of reduced-order modeling for controlling all types of transitioning and turbulent shear flows. Literally dozens of papers were published by him and his collaborators at several universities in Europe and the United States. It suffices here to cite one review paper that references many of Noack's papers [205].

5.3.2. Attractor dimension. Additional to the reductionist viewpoint exemplified by the work of Aubry et al. [125], Berkooz et al. [127], and Noack [205], attempts have been made to determine directly the dimension of the attractors underlying specific turbulent flows. Again, the central issue here is whether or not turbulent solutions to the infinite-dimensional Navier–Stokes equations can be asymptotically described by a finite number of degrees of freedom. Grappin and Lèorat [206] computed the Lyapunov exponents and the attractor dimensions of two- and three-dimensional periodic turbulent flows without shear. They found that the number of degrees of freedom contained in the large scales establishes an upper bound for the dimension of the attractor. Sirovich and Deane [207, 208] numerically determined the number of dimensions needed to specify chaotic Rayleigh-Bènard convection over a moderate range of Rayleigh numbers, Ra. They suggested that the intrinsic attractor dimension is $O\left[Ra^{2/3}\right]$.

The corresponding dimension in wall-bounded flows appears to be dauntingly high. Keefe et al. [209] determined the dimension of the attractor underlying turbulent Poiseuille flows with spatially periodic boundary conditions. Using a coarse-grained numerical simulation, they computed a lower bound on the Lyapunov dimension of the attractor to be approximately 352 at a pressure-gradient Reynolds number of 3,200. Keefe et al. argued that the attractor dimension in fully-resolved turbulence is unlikely to be much larger than 780. This suggests that periodic turbulent shear flows are deterministic chaos and that a strange attractor does underlie solutions to the Navier–Stokes equations. Temporal unpredictability in the turbulent Poiseuille flow is thus due to the exponential spreading property of such attractors. Although finite, the computed dimension invalidates the notion that the global turbulence can be attributed to the interaction of a 'few' degrees of freedom. Moreover, in a physical channel or boundary layer, the flow is not periodic and is open. The attractor dimension in such cases is not known but is believed to be even higher than the estimate provided by Keefe et al. for the periodic (quasi-closed) flow.

In contrast to closed, absolutely unstable flows (such as Taylor–Couette systems) where the number of degrees of freedom can be small, local measurements in open, convectively unstable flows (such as boundary layers) do not express the global dynamics, and the attractor dimension in that case

may inevitably be too large to be determined experimentally. According to the estimate provided by Keefe et al. [209], the colossal data required (about 10^D, where D is the attractor dimension) for measuring the dimension simply exceeds current computer capabilities. Turbulence near transition or near a wall is an exception to that bleak picture. In those special cases, a relatively small number of modes are excited and the resulting simple turbulence can therefore be described by a dynamical system of a more reasonable number of degrees of freedom.

5.3.3. Chaos control. There is another question of greater relevance here. Given a dynamical system in the chaotic regime, is it possible to stabilize its behavior through some kind of active control? While other alternatives have been devised [210–213] the method proposed by workers at the University of Maryland [214–221] promises to be a significant breakthrough. Comprehensive reviews and bibliographies of the emerging field of chaos control can be found in References [199, 222–225].

Ott et al. [214] demonstrated, through numerical experiments with the Hènon map, that it is possible to stabilize a chaotic motion about any pre-chosen, unstable orbit through the use of relatively small perturbations. The procedure consists of applying minute time-dependent perturbations to one of the system parameters to control the chaotic system around one of its many unstable periodic orbits. In this context, targeting refers to the process whereby an arbitrary initial condition on a chaotic attractor is steered toward a prescribed point (target) on this attractor. The goal is to reach the target as quickly as possible using a sequence of small perturbations [226].

The success of the Ott–Grebogi–Yorke's (OGY) strategy for controlling chaos hinges on the fact that beneath the apparent unpredictability of a chaotic system lies an intricate but highly ordered structure. Left to its own recourse, such a system continually shifts from one periodic pattern to another, creating the appearance of randomness. An appropriately controlled system, on the other hand, is locked into one particular type of repeating motion. With such reactive control the dynamical system becomes one with a stable behavior. The state of the system is represented as the intersection of a stable manifold and an unstable one. The control is applied intermittently whenever the system departs from the stable manifold by a prescribed tolerance; otherwise the control is shut off. The control attempts to put the system back onto the stable manifold so that the state converges toward the desired trajectory. Un-modeled dynamics cause noise in the system and a tendency for the state to wander off in the unstable direction. The intermittent control prevents that, and hence the desired trajectory is achieved. This efficient control is not unlike trying to balance a ball in the center of a horse saddle [185]. There is one stable direction (front/back) and one unstable direction (left/right). In the words of Moin and Bewley [185], the restless horse is the un-modeled dynamics, intermittently causing the ball to move in the wrong direction. The OGY's control needs only be applied, in the most direct manner possible, whenever the ball wanders off in the left/right direction.

The OGY's method has been successfully applied in a relatively simple experiment conducted by Ditto and colleagues at the Naval Surface Warfare Center [227, 228]. Therein, reverse chaos was obtained in a parametrically driven, gravitationally buckled, amorphous magnetoelastic ribbon. Garfinkel et al. [229] applied the same control strategy to stabilize drug-induced cardiac arrhythmias in sections of a rabbit ventricle. Other extensions, improvements, and applications of the OGY's strategy include higher-dimensional targeting [230, 231], controlling chaotic scattering in Hamiltonian (i.e., nondissipative, area conservative) systems [232, 233], synchronization of identical chaotic systems that govern communication, neural, or biological processes [234], use of chaos to transmit information [235, 236], control of transient chaos [237], and taming spatio-temporal chaos using a sparse array of controllers [238–240].

In a more complex system, such as a turbulent boundary layer, there exist numerous interdependent modes and many stable as well as unstable manifolds (directions). The flow can then be modeled as coherent structures plus a parameterized turbulent background. The proper orthogonal decomposition (POD) is used to model the coherent part because POD guarantees the minimum number of degrees of freedom for a given model accuracy. Factors that make turbulence control a challenging task are the potentially quite large perturbations caused by the un-modeled dynamics of the flow, the non-stationary nature of the desired dynamics, and the complexity of the saddle shape describing the dynamics of the different modes. Nevertheless, the OGY's control strategy has several advantages that are of special interest in the control of turbulence: (i) the mathematical model for the dynamical system need not be known; (ii) only small changes in the control parameter are required; and (iii) noise, with concomitant penalty, can be tolerated.

Keefe [241, 242] made a useful comparison between two nonlinear control strategies as applied to fluid problems. Ott–Grebogi–Yorke's feedback method described above and the model-based control strategy originated by Hübler, so-called H-method [211, 243]. Both novel control methods are essentially generalizations of the classical perturbation cancellation technique: apply a prescribed forcing to subtract the undesired dynamics and impose the desired one. The OGY's strategy exploits the sensitivity of chaotic systems to stabilize existing periodic orbits and steady states. Some feedback is needed to steer the trajectories toward the chosen fixed point, but the required control signal is minuscule. In contrast, Hübler's scheme does not explicitly make use of the system sensitivity. It produces general control response (periodic or aperiodic) and needs little or no feedback, but its control inputs are generally large. The OGY's strategy exploits the nonlinearity of a dynamical system. Indeed, the presence of a strange attractor and the extreme sensitivity of the dynamical system to initial conditions are essential to the success of that method. In contrast, the H-method works equally for both linear and nonlinear systems.

Keefe [241] first examined numerically the two schemes as applied to fully-developed and transitional solutions of the Ginzburg–Landau equation, an evolution equation that governs the initially weakly-nonlinear stages of transition in several flows and that possesses both transitional and fully-chaotic solutions. The Ginzburg–Landau equation has solutions that display either absolute or convective instabilities, and is thus

a reasonable model for both closed and open flows. Keefe's main conclusion is that control of nonlinear systems is best obtained by making maximum use possible of the underlying natural dynamics. If the goal dynamics is an unstable nonlinear solution of the equation and the flow is nearby at the instant control is applied, both methods perform reliably and at low-energy cost in reaching and maintaining this goal. Predictably, the performance of both control strategies degrades due to noise and the spatially discrete nature of realistic forcing. Subsequently, Keefe [241] extended the numerical experiment in an attempt to reduce the drag in a channel flow with spatially periodic boundary conditions. The OGY's method reduces the skin friction to 60–80% of the uncontrolled value at a mass-flux Reynolds number of 4,408. The H-method fails to achieve any drag reduction when starting from a fully-turbulent initial condition but shows potential for suppressing or retarding laminar-to-turbulence transition. Keefe suggested that the H-strategy might be more appropriate for boundary layer control, while the OGY's method might best be used for channel flows [241].

It is also relevant here to note the work of Bau and his colleagues at the University of Pennsylvania [244, 245], who devised a feedback control to stabilize (relaminarize) the naturally occurring chaotic oscillations of a toroidal thermal convection-loop heated from below and cooled from above. Based on a simple mathematical model for the thermosyphon, Bau and his colleagues constructed a reactive control system that was used to alter significantly the flow characteristics inside the convection loop. Their linear control strategy, perhaps a special version of the OGY's chaos control method, consists simply of sensing the deviation of fluid temperatures from desired values at a number of locations inside the thermosyphon loop and then altering the wall heating either to suppress or to enhance such deviations. Wang et al. [245] also suggested extending their theoretical and experimental method to more complex situations such as those involving Bènard convection [246, 247]. Hu and Bau [248] used a similar feedback control strategy to demonstrate that the critical Reynolds number for the loss of stability of planar Poiseuille flow can be significantly increased or decreased.

Other attempts to use low-dimensional dynamical systems representation for flow control include the work of Berkooz et al. [196], Corke et al. [249], and Coller et al. [250, 251]. Berkooz et al. [196] applied techniques of modern control theory to estimate the phase-space location of dynamical models of the wall-layer coherent structures, and used these estimates to control the model dynamics. Since discrete wall-sensors provide incomplete knowledge of phase-space location, Berkooz et al. maintain that a nonlinear observer, which incorporates past information and the equations of motion into the estimation procedure, is required. Using an extended Kalman filter, they achieved effective control of a bursting pair of rolls with the equivalent of two wall-mounted shear sensors.

Corke et al. [249] used a low-dimensional dynamical system based on the proper orthogonal decomposition to guide control experiments for an axisymmetric jet. By sensing the downstream velocity and actuating an array of miniature speakers located at the lip of the jet, their feedback control succeeded in converting the near-field instabilities from spatial-convective to temporal-global.

Coller et al. [250, 251] developed a feedback control strategy for strongly nonlinear dynamical systems, such as turbulent flows, subject to small random perturbations that kick the system intermittently from one saddle point to another along heteroclinic cycles. In essence, their approach is to use local, weakly-nonlinear feedback control to keep a solution near a saddle point as long as possible, but then to let the natural, global nonlinear dynamics run its course when bursting (in a low-dimensional model) does occur. Though conceptually related to the OGY's strategy, Coller et al.'s method does not actually stabilize the state but merely holds the system near the desired point longer than it would stay otherwise.

Shinbrot and Ottino [252, 253] offer yet another strategy presumably most suited for controlling coherent structures in area-preserving turbulent flows. Their geometric method exploits the premise that the dynamical mechanisms that produce the organized structures can be remarkably simple. By repeated stretching and folding of 'horseshoes' that are present in chaotic systems, Shinbrot and Ottino have demonstrated numerically as well as experimentally the ability to create, destroy, or manipulate coherent structures in chaotic fluid systems. The key idea to create such structures is to intentionally place folds of horseshoes near low-order periodic points. In a dissipative dynamical system, volumes contract in state space and the co-location of a fold with a periodic point leads to an isolated region that contract asymptotically to a point. Provided that the folding is done properly, it counteracts stretching. Shinbrot and Ottino [252] applied the technique to three prototypical problems: (i) a one-dimensional chaotic map; (ii) a two-dimensional one; and (iii) a chaotically advected fluid. Shinbrot and colleagues [221, 224, 254] provide reviews of the stretching/folding as well as other chaos control strategies.

5.4. Soft computing. In this and the following subsection, we discuss the applicability of soft-computing tools to reactive flow control. The term soft computing was coined by the mathematician/computer scientist Lotfi Zadeh of the University of California, Berkeley, to describe several ingenious modes of computations that exploit tolerance for imprecision and uncertainty in complex systems to achieve tractability, robustness, and low cost [255–258]. The principle of complexity provides the impetus for soft computing: as the complexity of a system increases, the ability to predict its response diminishes until a threshold is reached beyond which precision and relevance become almost mutually exclusive [259]. In other words, precision and certainty carry a cost. By employing modes of reasoning—probabilistic reasoning—that are approximate rather than exact, soft computing can help in searching for globally optimal design or in achieving effectual control while taking into account system uncertainties and risks.

Soft computing refers to a domain of computational intelligence that loosely lies in between purely numerical (hard) computing and purely symbolic computations. Alternatively, one can think about symbolic computations as a form of arti-

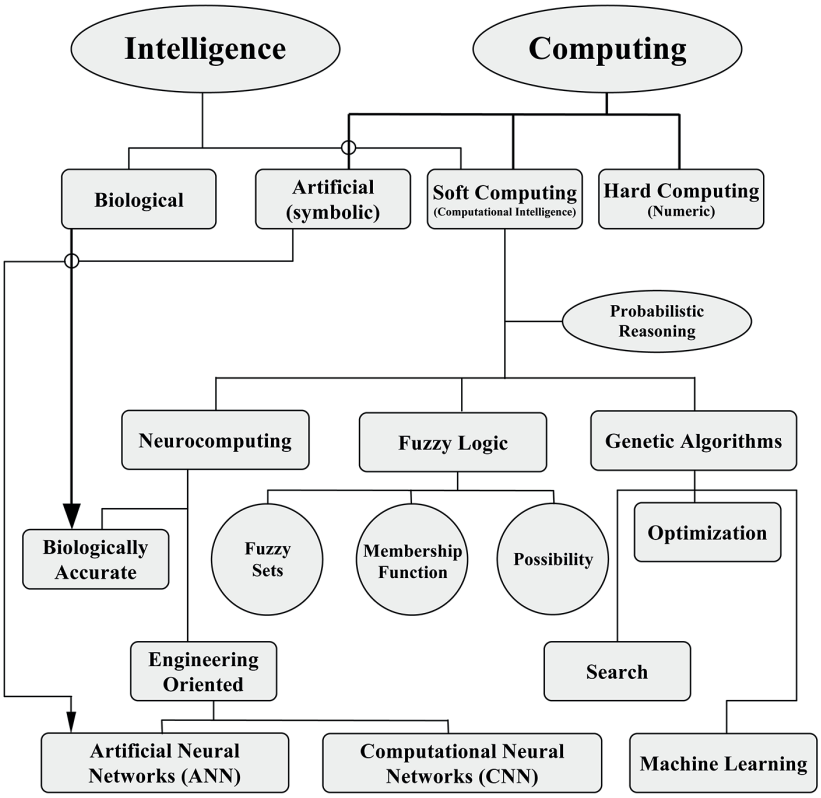

Fig. 13. Tools for soft computing. Block diagram adapted from Gad-el-Hak [102]

ficial intelligence lying in between biological intelligence and computational intelligence (soft computing). The schematic in Fig. 13 illustrates the general idea. Artificial intelligence relies on symbolic information processing techniques and uses logic as representation and inference mechanisms. It strives to approach the high level of human cognition. In contrast, soft computing is based on modeling low-level cognitive processes and strongly emphasizes modeling of uncertainty as well as learning. Computational intelligence mimics the ability of the human's brain to employ modes of reasoning that are approximate. Soft computing provides machinery for the numeric representation of the types of constructs developed in the symbolic artificial intelligence. The boundaries between these paradigms are of course fuzzy.

The principal constituents of soft computing are neurocomputing, fuzzy logic, and genetic algorithms, as depicted in Fig. 13. These elements, together with probabilistic reasoning, can be combined in hybrid arrangements resulting in better systems in terms of parallelism, fault tolerance, adaptivity, and uncertainty management. The block diagram in that figure is *not* a family tree: a particular block is not necessarily the offspring of the one above it. For example, machine learning and artificial intelligence are overarching principles and include, among other things, genetic algorithms. Also, a genetic algorithm solves an optimization problem, and not the other way around. The limited use of arrows in Fig. 13 is therefore intentional, and the block diagram is for illustrative purposes only, and therefore should not be taken literally.

Neurocomputing, fuzzy logic, and genetic algorithms have been employed for fluid flow to construct powerful controllers. All three softcomputing tools have been utilized in other fields as well, for example in large-scale subway controllers and in video cameras. A brief description of those three constituents follows.

Neurocomputing is inspired by the neurons of the human's brain and how they work. Neural networks are information processing devices that can learn by adapting synaptic weights to changes in the surrounding environment, can handle imprecise, fuzzy, noisy, and probabilistic information, and can generalize from known tasks (examples) to unknown ones. Actual engineering oriented hardware is termed artificial neural networks (ANN), while algorithms are called computational neural networks (CNN). The nonlinear, highly parallel networks can perform any of the following tasks: classification, pattern matching, optimization, control, and noise removal. As modeling and optimization tools, neural networks are particularly useful when good analytic models are either unknown or extremely complex.

An artificial neural network consists of a large number of highly interconnected processing elements—essentially equations known as "transfer functions" that are analogous to neurons. Those elements are tied together with weighted connections that are analogous to synapses. A processing unit takes weighted signals from other units, possibly combines them, and gives a numeric result.

The behavior of neural networks—how they map input data—is influenced primarily by the transfer functions of the

processing elements, how the transfer functions are interconnected, and the weights of those interconnections. Learning typically occurs by example through exposure to a set of input–output data, where the training algorithm adjusts the connection weights (synapses). These connection weights store the knowledge necessary to solve specific problems. As an example, it is now possible to use neural networks to sense (smell) odors in many different applications [260]. The electronic noses (e-noses) are finding commercial applications in medical diagnostics, environmental monitoring, and the processing and quality control of foods. Neural networks as used in fluid flow control will be covered in the following subsection.

Fuzzy logic was introduced by Lotfi Zadeh in 1965 as a mathematical tool to deal with uncertainty and imprecision. The book by Yager and Zadeh [255] is an excellent primer to the field. For computing and reasoning, general concepts such as size are implemented into a computer algorithm by using mostly words such as small, medium, or large. Fuzzy logic, therefore, provides a unique methodology for computing with words. Its rationalism is based on three mathematical concepts: fuzzy sets, membership function, and possibility. As dictated by a membership function, fuzzy sets allow a gradual transition from 'belonging' to 'not belonging' to a set. The concept of possibility provides a mechanism for interpreting factual statements involving fuzzy sets. Three processes are involved in solving a practical problem using fuzzy logic: fuzzification, analysis, and defuzzification. Given a complex, unsolvable problem in real space, those three steps involve enlarging the space into a virtual one, searching for a solution in the new superset, then specializing this solution to the original real constraints.

Genetic algorithms are search algorithms based loosely on the mechanics of natural selection and natural genetics. They combine survival of the fittest among string structures with structured yet randomized information exchange, and are used for search, optimization, and machine learning. For control, genetic algorithms aim at achieving minimum cost function and maximum performance measure while satisfying the problem constraints. The books by Goldberg [261], Davis [262], and Holland [263] provide gentle introduction to the field.

In the Darwinian principle of natural selection, the fittest members of a species are favored to produce offspring. Even biologists cannot help but being awed by the complexity of life observed to evolve in the relatively short time suggested by the fossil records. A living being is an amalgam of characteristics determined by the (typically tens of thousands) genes in its chromosomes. Each gene may have several forms or alternatives called alleles that produce differences in the set of characteristics associated with that gene. The chromosomes are therefore the organic devices through which the structure of a creature is encoded, and this living being is created partly through the process of decoding those chromosomes. Genes transmits hereditary characters and form specific parts of a self-perpetuated deoxyribonucleic acid (DNA) in a cell nucleus. Natural selection is the link between the chromosomes and the performance of their decoded structures. Simply put, the process of natural selection causes those chromosomes that encode successful structures to reproduce more often than those that do not.

In an attempt to solve difficult problems, John H. Holland of the University of Michigan introduced in the early 1970s the manmade version of the procedure of natural evolution. The candidate solutions to a problem are ranked by the genetic algorithm according to how well they satisfy a certain criterion, and the fittest members are the most favored to combine amongst themselves to form the next generation of the members of species. Fitter members presumably produce even fitter offspring and therefore better solutions to the problem at hand. Binary strings represent solutions, and each trial solution is coded as a vector called chromosome. The elements of a chromosome are described as genes, and its varying values at specific positions are called alleles. Good solutions are selected for reproduction based on a fitness function using genetic recombination operators such as crossover and mutation.

The main advantage of genetic algorithms is their global parallelism in which the search efforts to many regions of the search area are simultaneously allocated. Genetic algorithms have been used for the control of different dynamical systems, as for example the optimization of robot trajectories. But to my knowledge, the control of turbulent flows is yet to benefit fully from this powerful soft-computing tool. In particular, when a finite number of sensors are used to gather information about the state of the flow, a genetic algorithm perhaps combined with a neural network can adapt and learn to use current information to eliminate the uncertainty created by insufficient sensed information.

5.5. Neural network for flow control. Biologically inspired neural networks are finding increased applications in many fields of science and technology. Modeling of complex dynamical systems, adaptive noise canceling in telephones and modems, bomb sniffers, mortgage-risk evaluators, sonar classifiers, word recognizers, and smartphones are but a few of existing usage of neural nets. The book by Nelson and Illingworth [264] provides a lucid introduction to the field, and the review article by Antsaklis [265] focuses on the use of neural nets for the control of complex dynamical systems. For flow control applications, neural networks offer the possibility of adaptive controllers that are simpler and potentially less sensitive to parameter variations as compared to conventional controllers. Moreover, if a colossal number of sensors and actuators are to be used, the massively parallel computational power of neural nets will surely be needed for real-time control.

The basic elements of a neural network are input layer, hidden layers, and output layer. Several inputs are connected to the nodes (neurons or processing elements) that form the input layer. There are one or more hidden layers, followed by an output layer. Note that the number of connections is higher than the total number of nodes. Both numbers are chosen based on the particular application and can be arbitrarily large for complex tasks. Simply put, the multi-task—albeit simple—job of each processing element is to evaluate each of the input signals to that particular element, calculate the weighted sum of the combined inputs, compare that total to some threshold

level, and finally determine what the output should be. The various weights are the adaptive coefficients that vary dynamically as the network learns to perform its assigned task; some inputs are more important than others. The threshold, or transfer function, is generally nonlinear. The most commonly used transfer function is the continuous sigmoid, or S-shaped, curve, which approaches a minimum and maximum value at the asymptotes. If the sum of the weighted inputs is larger than the threshold value, the neuron generates a signal; otherwise no signal is fired. Neural networks can operate in feedforward or feedback mode. Complex systems for which the dynamical equations may not be known or may be too difficult to solve can be modeled using neural nets.

For flow control, neural networks provide convenient, fast, nonlinear adaptive algorithms to relate sensor outputs to actuator inputs via variable-coefficient functions and nonlinear, sigmoid saturation functions. With no prior knowledge of the pertinent dynamics, a self-learning neural network develops a model for that dynamics through observations of the applied control and sensed measurements. The network is by choice nonlinear and can therefore better handle nonlinear dynamical systems, a difficult task when classical (linear or weakly nonlinear) control strategies are attempted. The feedforward type of neural networks acts as a nonlinear filter forming an output from a set of input data. The output can then be compared to some desired output, and the difference (error) is typically used in a back-propagation algorithm that updates the network parameters.

The number of researchers using neural networks to control fluid flows is growing rapidly. In here, we provide only a small sample. Using a pre-trained neural network, Fan et al. [165] conducted a conceptual reactive flow control experiment to delay laminar-to-turbulence transition. Numerical simulations of their flow control system demonstrate almost complete cancellation of single and multiple artificial wave disturbances. Their controller was used in a wind-tunnel experiment and successfully attenuated natural-disturbance signals from a developing wave packet.

Jacobson and Reynolds [161, 163, 164] used neural networks to minimize the boundary velocity gradient of three model flows: (i) the one-dimensional stochastic Burgers equation; (ii) a two-dimensional computational model of the near-wall region of a turbulent boundary layer; and (iii) a real-time turbulent flow with a spanwise array of wall actuators together with upstream and downstream wall-sensors. For all three numerical problems, the neural network successfully learned about the flow and developed into proficient controllers. For the laboratory experiments, however, Jacobson and Reynolds [163] report that the neural network training time was much longer and the performance was no better than a simpler ad hoc controller that they developed. Jacobson and Reynolds emphasize that alternative neural net configurations and convergence algorithms may, however, greatly improve the network performance.

Using the angle of attack and angular velocity as inputs, Faller et al. [266] trained a neural network to model the measured unsteady surface pressure over a pitching airfoil [267]. Following training and using the instantaneous angle of attack and pitch rate as the only inputs, their network was able to accurately predict the surface pressure topology as well as the time-dependent aerodynamic forces and moments. The model was then used to develop a neural network controller for wing-motion actuator signals, which in turn provided direct control of the lift-to-drag ratio across a wide range of time-dependent motion histories.

Kawthar-Ali and Acharya [268] developed a neural network controller for use in suppressing the dynamic-stall vortex that periodically develops in the leading edge of a pitching airfoil. Based on the current state of the unsteady pressure field, their control system specified the optimum amount of leading-edge suction to achieve complete vortex suppression.

As a final example, Lee et al. [269] constructed, trained, and applied an adaptive controller based on a neural network to reduce the skin-friction drag in a turbulent channel flow. The numerical experiments were conducted in the rather low-Reynolds-number (based on friction velocity and channel half-height) of $a^+ = 100$. The authors report approximately 20% drag reduction.

6. Progress in closed-loop control during the third millennial

Thus far, this article focused on the history of coherent structures and reactive flow control up to the year 2000. The field of closed-loop flow control witnessed its renaissance and, simultaneously, its formative years during the period 1980–2000. The first two decades of the third millennial witnessed explosive growth in the field of adaptive flow control. A Google Scholar's search—restricted to the years 2000–2018—using the phrase "closed-loop flow control" yielded close to 300,000 hits (1 May 2018). "Adaptive flow control" yielded close to 1,700,000 hits, during the same period. Of course not all of those hits are serious publications. Nevertheless, the historical nature of the present article precludes adequate coverage of the most recent literature in closed-loop flow control. That monumental task is left to another occasion, but herein we provide a handful of highlights.

Of note are the four meetings held at the Technical University of Berlin and the resulting proceedings published by Springer [270–273]. The meetings were organized by Rudibert King in 2006, 2010, 2014, and 2018, and entitled "Active Flow Control" (title later broadened to"Active Flow and Combustion Control"). Several similar conferences are organized annually around the world.

The *AIAA Journal* is dedicating an entire issue to the subject of flow control, scheduled to be published in 2018. The guest editors of that special issue are David Greenblatt, Israel J. Wygnanski, and Edward A. Whalen.

Other publications worth noting are the review paper by Krishnan et al. [274], in which the authors extensively discuss the latest development in hybrid laminar flow control systems (a combination of passive flow control and predetermined, open-loop, active control); the article by Kornilov & Boiko [275], in which the authors review the advances and challenges

of periodic forcing of the turbulent boundary layer on a body of revolution; and the paper cited earlier by Brunton and Noack [205], in which the authors review the progress and challenges of closed-loop turbulence control, with a focus on artificial intelligence/machine-learning control (AI/MLC). Between those three papers, there are 634 cited references.

Other significant recent publications include the work of John Kim [276, 277] who applies linear optimal control theory to reduce the skin-friction drag in turbulent boundary layers. Kim shows that singular-value decomposition analysis of the linear system allows the examination of different approaches to boundary layer control without carrying out the rather expensive (in computer time) nonlinear simulations.

Nobuhide Kasagi and colleagues [278] propose a theoretical framework that may enable laboratory-scale drag-reduction methods to be extended to flight-scale Reynolds numbers. Their scheme utilizes a virtual active feedback control system. Dan Henningson and colleagues [279–281] propose a transition-delay methodology that utilizes feedback, closed-loop control. Their work emphasizes the important role of sensors and actuators. The last paper is an extensive review—citing 96 references—of adaptive and model-based control theory as applied to convectively unstable flows.

The *Journal of Fluid Mechanics* quite recently published two rather lengthy perspectives [282, 283] on scale interactions and coherent structures in turbulent boundary layers. As indicated in Section 5, coherent structures' identification is the key to successful open-loop and closed-loop reactive control.

Finally, the use of machine learning tools has witnessed explosive growth during the last two decades. Petros Koumoutsakos and his group used Rechenberg–Schwefel evolutionary algorithms for the optimization of noisy combustion processes [284] as well as to reduce the time complexity of derandomized evolution strategies [285]. A recent book [286] and a proceedings article [286] are devoted to machine learning, closed-loop control, and taming nonlinear dynamics and turbulence.

We end this section with a look through the crystal ball. The above is a small sample of the extensive literature in open- and closed-loop control for laminar, transitioning, and turbulent boundary layers. The question of field applications is a natural one: why aren't we seeing reactive flow control in actual airplanes and submarines, despite the thousands of basic-research papers published? The answer is we do, but on a limited scale. Closed-loop control of combustion instabilities, separation in engine inlets, noise cancellation, and control of micro air vehicles do exist in actual applications (see, for example, the special issue of *AIAA Journal* mentioned earlier in this section). But skin-friction-reduction applications to the transitioning or turbulent boundary layers on the wing, nacelle, or fuselage of commercial aircraft are yet to be realized.

Herein, I offer a personal view. Boeing invests around $1 billion to develop a new wing, void of any sensors and actuators. It would probably cost an order of magnitude higher price tag to develop a 'smart' wing, with millions of affordable microsensors and microactuators working and communicating in extreme environments. Would the airlines be willing to pay for the increased up-front cost, even if the fuel savings over a ten-year period, say, would more than compensate? No one knows the answer to that and it would take a courageous, forward-looking executive to take the risk. The government, especially under the current political climate, most certainly wont be willing to offer the huge investment needed, even to at least mitigate the climate-change challenges.

I am reminded with the Texas Instruments' visionary executive who made the bold decision to invest in developing the digital micromirror device (DMD). Such device has one million or more 16×16 μm individually addressable mirrors. Each 'actuator' is capable of rotating $\pm10°$. TA invested close to $1 billion to develop an affordable DMD, which costs around 100, and is now used worldwide in PC projectors, video walls, HDTVs, and digital cinemas. The company sells enough of the micromirros to make up for the initial development cost. But no one knew that when the decision to carry out the expensive ten-year development project was made in the 1970s.

7. Concluding remarks

The field of flow control is broad, practically very important, and rich in scientific and technological challenges. Though as old as human's ancestors, the field's potential for improving our lives may keep it going strong for yet another millennium. Herein, I have made a modest attempt to place the field in a unifying framework and to properly categorize the different control strategies. At a minimum, I hope to have provided a useful navigation tool through the colossal literature in the field of flow control and its intricately related subfields such as transitioning and turbulent flows, coherent structures, reactive control, control theory, chaos, microelectromechanical systems, and soft computing.

There is no lack of flow control methods to achieve a particular goal for free-shear or wall-bounded flows across the entire range of Mach and Reynolds numbers. Ranging from simple to complex, from inexpensive to expensive, from passive to active to reactive, and from market ready to futuristic, the fluids engineer has a great variety of control devices to choose from. Flow control is most effective when applied near the transition or separation points; in other words, near critical flow regimes where flow instabilities magnify quickly. Therefore, delaying/advancing laminar-to-turbulence transition and preventing/provoking separation can readily be accomplished. To reduce the skin-friction drag in a non-separating turbulent boundary layer, where the mean flow is quite stable, is a more challenging problem. In all cases, since flow control goals are often adversely interrelated, constrained-design compromises are always in the forefront. When designing a flow control device to achieve a particular goal such as skin-friction reduction, the engineer's foremost task is to ensure a minimum and most benign tradeoff.

Market-ready techniques include passive and predetermined active control. Shaping, suction, heating/cooling, Lorentz body force, and compliant coatings can be used to delay transition by an order of magnitude in Reynolds number, and can also be used to prevent boundary layer separation. The use of polymers, microbubbles, riblets, and large-eddy breakup devices (LEBUs)

can lead to skin-friction reduction in turbulent boundary layers. Numerous other techniques are available to reduce form drag, induced drag, and wave drag. Remaining issues for field application of market-ready techniques include cost, maintenance, and reliability. Potential further improvements in classical flow control techniques will perhaps involve combining more than one technique aiming at achieving a favorable effect that is greater than the sum. Examples include combining suction or polymer injection with riblets for increased effectiveness and saving. Due to its obvious difficulties, synergism has not been extensively studied in the past but deserves future considerations.

Classical control techniques, though spectacularly successful in the past, have been extended to near their physical limits. Conventional strategies are often ineffective for turbulent flows. Substantial gains are potentially possible, however, when reactive flow control methods are used to target specific coherent structures for modulation. Particularly for wall-bounded turbulent flows, reactive control requires large number of sensors and actuators and will not become practical until the technology for manufacturing inexpensive, robust microsensors and microactuators becomes available. Autonomous control algorithms and associated computers to handle the required colossal data in real time must also be developed. Further research is needed in dynamical systems theory particularly chaos control, microelectromechanical systems (MEMS), and alternative neural network configurations, convergence algorithms, and distributed control. The difficulties are daunting but the potential payoffs are enormous.

The present essay emphasized the frontiers of the field of control of turbulent flows, reviewing the important advances that took place during the past few decades and providing a blueprint for future progress. In two words, the future of flow control is in taming turbulence by targeting its coherent structures: "reactive control". Recent developments in chaos control, microfabrication, and soft-computing tools are making it more feasible to perform reactive control of turbulent flows to achieve drag reduction, lift enhancement, mixing augmentation, and noise suppression. Field applications, however, have to await further progress in those three modern areas.

In parting, it may be worth recalling that a mere 10% reduction in the total drag of an aircraft translates into a saving of 3.5-billion dollars in annual fuel cost for the commercial fleet of airplanes in the United States alone. Globally, the aviation industry gave rise to $\approx 2\%$ of all human-induced carbon-dioxide emissions. Contrast the potential benefits to the annual worldwide expenditure of perhaps a few million dollars for all basic research in the broad field of flow control. Applied and translational research and development, mostly a domain of the private sector, are now needed. High-risk R&D is calling the next Steve Jobs, Bill Gates, or Elon Musk.

Taming turbulence, though arduous, will pay for itself in gold. Reactive control as difficult as it seems, is neither impossible nor a pie in the sky. Beside, lofty goals require strenuous efforts. Easy solutions to difficult problems are likely to be misguided as intimated by the essayist Henry Louis Mencken's famous quote, "There is always an easy solution to every human problem—neat, plausible and wrong." As for the future? The French pilot, warrior, and author Antoine de Saint-Exupèry wrote in *Citadelle* (translated into English as *The Wisdom of the Sands*): "As for the future, your task is not to foresee, but to enable it."

References

[1] T. Weis-Fogh and M. Jensen, "Biology and Physics of Locust Flight. I. Basic Principles in Insect Flight. A Critical Review," *Philo. T. R. Soc. B* 239, 415–458 (1956).
[2] M.J. Lighthill, "On the Weis-Fogh Mechanism of Lift Generation," *J. Fluid Mech*. 60, 1–17 (1973).
[3] K.D. Jones, C.M. Dohring, and M.F. Platzer, "Experimental and Computational Investigation of the Knoller–Betz Effect," *AIAA J.* 36, 1240–1246 (1998).
[4] K.D. Jones and M.F. Platzer, "Bio-Inspired Design of Flapping Wings Micro Air Vehicles–an Engineer's Perspective," *AIAA Paper* No. 2006–0037, Reston, Virginia, 2006.
[5] M.F. Platzer, "Integrated Propulsion/Lift/Control System for Aircraft and Ship Applications," United States Patent No. 5, 975, 462, 1999.
[6] H.T. Banks, R.C. Smith, and Y. Wang, *Smart Material Structures: Modeling, Estimation and Control*, Wiley, New York, 1996.
[7] M. Schwartz, editor, *Encyclopedia of Smart Materials*, vols. 1 and 2, Wiley-Interscience, New York, 2002.
[8] G.M. Atkinson and O. Zoubeida, "Polymer Microsystems: Materials and Fabrication," in *The MEMS Handbook*, ed. M. Gadel- Hak, vol. II, pp. 9.1–9.36, CRC Taylor&Francis, Boca Raton, Florida, 2006.
[9] H. Lamb, *Hydrodynamics*, second edition, Cambridge University Press, Cambridge, Great Britain, 1895.
[10] J.L. Lumley, "Turbulence and Turbulence Modeling," in *Research Trends in Fluid Dynamics*, eds. J.L. Lumley, A. Acrivos, L.G. Leal, and S. Leibovich, pp. 167–177, American Institute of Physics, Woodbury, New York, 1996.
[11] H.W. Liepmann, "The Rise and Fall of Ideas in Turbulence," *American Scientist* 67, no. 2, 221–228 (1979).
[12] J.C.R. Hunt, D.J. Carruthers, and J.C.H. Fung, "Rapid Distortion Theory as a Means of Exploring the Structure of Turbulence," in *New Perspectives in Turbulence*, ed. L. Sirovich, pp. 55–103, Springer-Verlag, Berlin, 1991.
[13] M. Gad-el-Hak, "Splendor of Fluids in Motion," *Prog. Aerosp. Sci*. 29, 81–123 (1992).
[14] E. MacCurdy, *The Notebooks of Leonardo da Vinci*, vol. I and II, Reynal & Hitchcock, New York, 1938.
[15] J.L. Lumley, "Some Comments on Turbulence," *Phys. Fluids A* 4, 203–211 (1992).
[16] O. Reynolds, "An Experimental Investigation of the Circumstances which Determine Whether the Motion of Water shall be Direct or Sinuous, and of the Law of Resistance in Parallel Channels," *Phil. Trans. Roy. Soc. Lond. A* 174, 935–982 (1883).
[17] O. Reynolds, "On the Dynamical Theory of Incompressible Viscous Fluids and the Determination of the Criterion," *Phil. Trans. Roy. Soc. Lond. A* 186, 123–164 (1895).
[18] J.L. Lumley, "Turbulence Modeling," *J. Appl. Mech*. 50, 1097–1103 (1983).
[19] J.L. Lumley, "Turbulence Modeling," *Proc. Tenth U.S. National Cong. of Applied Mechanics*, ed. J. P. Lamb, pp. 33–39, ASME, New York, 1987.

[20] C.G. Speziale, "Analytical Methods for the Development of Reynolds-Stress Closures in Turbulence," *Annu. Rev. Fluid Mech*. 23, 107–157 (1991).
[21] D.C. Wilcox, *Turbulence Modeling for CFD*, DCW Industries, Los Angeles, California, 1993.
[22] A.K.M.F. Hussain, "Coherent Structures and Turbulence," *J. Fluid Mech*. 173, 303–356 (1986).
[23] J.T.C. Liu, "Contributions to the Understanding of Large-Scale Coherent Structures in Developing Free Turbulent Shear Flows," in *Advances in Applied Mechanics*, eds. J. W. Hutchinson and T. Y. Wu, vol. 26, pp. 183–309, Academic Press, Boston, Massachusetts, 1988.
[24] H.L. Dryden, "Recent Advances in the Mechanics of Boundary Layer Flow," in *Advances in Applied Mechanics*, eds. R. von Mises and Th. von Kármán, vol. 1, pp. 1–40, Academic Press, Boston, Massachusetts, 1948.
[25] H.W. Liepmann, "Aspects of the Turbulence Problem. Part II," *Z. Angew. Math. Phys*. 3, 407–426 (1952).
[26] A.A. Townsend, *The Structure of Turbulent Shear Flow*, Cambridge University Press, Cambridge, Great Britain, 1956.
[27] G. Haller, "An Objective Definition of a Vortex," *J. Fluid Mech*. 525, 1–26 (2005).
[28] M. Serra and G. Haller, "Forecasting Long-Lived Lagrangian Vortices From Their Objective Eulerian Footprints," *J. Fluid Mech*. 813, 436–457 (2017).
[29] J. Kasten, J. Reininghaus, I. Hotz, H.-C. Hege, B. R. Noack, G. Daviller, and M. Morzyński, "Acceleration Feature Points of Unsteady Shear Flows," *Arch. Mech*. 68, 55–80 (2016).
[30] H.W. Liepmann, "Free Turbulent Flows," *Mécanique de la Turbulence, Int. Symp. Nat. Sci. Res. Centre*, pp. 211–227, Marseille 1961, CNRS, Paris, France, 1962.
[31] G.L. Brown and A. Roshko, "The Effect of Density Difference on the Turbulent Mixing Layer," in *Turbulent Shear Flows*, pp. 23.1–23.12, AGARD-CP-93, Rhode-Saint-Génèse, Belgium, 1971.
[32] G.L. Brown and A. Roshko, "On Density Effects and Large Structure in Turbulent Mixing Layers," *J. Fluid Mech*. 64, 775–816 (1974).
[33] P. Holmes, J.L. Lumley, G. Berkooz, G., and C.W. Rowley, *Turbulence, Coherent Structures, Dynamical Systems and Symmetry*, second edition, Cambridge University Press, Cambridge, Great Britain, 2012.
[34] M.V. Wickerhauser, *Adapted Wavelet Analysis from Theory to Software*, A.K. Peters Ltd., Wellesley, Massachusetts, 1994.
[35] M. Farge, "Wavelet Transforms and Their Applications to Turbulence," *Annu. Rev. Fluid Mech*. 24, 395–457 (1992).
[36] O.V. Vasilyev, D.A. Yuen, and S. Paolucci, "Solving PDEs UsingWavelets," *Computers in Physics* 11, no. 5, 429–435 (1997).
[37] J. Laufer, "New Trends in Experimental Turbulence Research," *Annu. Rev. Fluid Mech*. 7, 307–326 (1975).
[38] A.A. Townsend, *The Structure of Turbulent Shear Flow*, second edition, Cambridge University Press, Cambridge, Great Britain, 1976.
[39] B.J. Cantwell, "Organized Motion in Turbulent Flow," *Ann. Rev. Fluid Mech*. 13, 457–515 (1981).
[40] H.E. Fiedler, "Coherent Structures in Turbulent Flows," *Prog. Aerosp. Sci*. 25, 231–269 (1988).
[41] S.K. Robinson, "Coherent Motions in the Turbulent Boundary Layer," *Annu. Rev. Fluid Mech*. 23, 601–639 (1991).
[42] J. Delville, L. Cordier, and J.-P. Bonnet, "Large-Scale-Structure Identification and Control in *Turbulent Shear Flows*," in Flow Control: Fundamentals and Practices, eds. M. Gad-el-Hak, A. Pollard, and J.-P. Bonnet, 199–273, Springer-Verlag, Berlin, 1998.
[43] J.L. Lumley, "Coherent Structures in Turbulence," in *Transition and Turbulence*, ed. R.E. Meyer, pp. 215–242, Academic Press, New York, 1981.
[44] M. Gad-el-Hak, R.F. Blackwelder, and J.J. Riley, "On the Growth of Turbulent Regions in Laminar Boundary Layers," *J. Fluid Mech*. 110, 73–95 (1981).
[45] H.E. Fiedler, "Control of Free Turbulent Shear Flows," in *Flow Control: Fundamentals and Practices*, eds. M. Gad-el-Hak, A. Pollard, and J.-P. Bonnet, pp. 335–429, Springer-Verlag, 1998, Berlin.
[46] A. Roshko, "Structure of Turbulent Shear Flows: a New Look," *AIAA J*. 14, 1349–1357 (1976).
[47] C.D. Winant and F.K. Browand, "Vortex Pairing: the Mechanism of Turbulent Mixing Layer Growth at Moderate Reynolds Numbers," *J. Fluid Mech*. 63, 237–255 (1974).
[48] A.A. Townsend, "Equilibrium Layers and Wall Turbulence," *J. Fluid Mech*. 11, 97–120 (1961).
[49] H.P. Bakewell and J.L. Lumley, "Viscous Sublayer and Adjacent Wall Region in Turbulent Pipe Flow," *Phys. Fluids* 10, 1880–1889 (1967).
[50] A.A. Townsend, "Entrainment and the Structure of Turbulent Flow," *J. Fluid Mech*. 41, 13–46 (1970).
[51] R.L. Panton, editor, *Self-Sustaining Mechanisms of Wall Turbulence*, Computational Mechanics Publications, Southampton, Great Britain, 1997.
[52] L.S.G. Kovasznay, "The Turbulent Boundary Layer," *Annu. Rev. Fluid Mech*. 2, 95–112 (1970).
[53] W.W. Willmarth, "Structure of Turbulence in Boundary Layers," *Adv. Appl. Mech*. 15, 159–254 (1975).
[54] W.W. Willmarth, "Pressure Fluctuations beneath Turbulent Boundary Layers," *Annu. Rev. Fluid Mech*. 7, 13–37 (1975).
[55] P.G. Saffman, "Problems and Progress in the Theory of Turbulence," in *Structure and Mechanisms of Turbulence II*, ed. H. Fiedler, pp. 273–306, Springer-Verlag, Berlin, 1978.
[56] H.E. Fiedler, "Coherent Structures," in *Advances in Turbulence*, eds. G. Comte-Bellot and J. Mathieu, pp. 320–336, Springer-Verlag, Berlin, 1986.
[57] R.F. Blackwelder, "Coherent Structures Associated with Turbulent Transport," in *Transport Phenomena in Turbulent Flows*, eds. M. Hirata and N. Kasagi, pp. 69–88, Hemisphere, New York, 1988.
[58] R.F. Blackwelder, "Some Notes on Drag Reduction in the Near-Wall Region," in *Flow Control: Fundamentals and Practices*, eds. M. Gad-el-Hak, A. Pollard and J.-P. Bonnet, pp. 155–198, Springer-Verlag, Berlin, 1998.
[59] M. Gad-el-Hak, R.F. Blackwelder, and J.J. Riley, "On the Interaction of Compliant Coatings with Boundary Layer Flows," *J. Fluid Mech*. 140, 257–280 (1984).
[60] R.E. Falco, "The Production of Turbulence Near aWall," AIAA Paper No. 80-l356, New York, 1980.
[61] J.J. Riley and M. Gad-el-Hak, "The Dynamics of Turbulent Spots," in *Frontiers in Fluid Mechanics*, eds. S.H. Davis and J.L. Lumley, pp. 123–155, Springer-Verlag, Berlin, 1985.
[62] L.S.G. Kovasznay, V. Kibens, V., and R.F. Blackwelder, "Large-Scale Motion in the Intermittent Region of a Turbulent Boundary Layer," *J. Fluid Mech*. 41, 283–325 (1970).
[63] R.F. Blackwelder and L.S.G. Kovasznay, "Time-Scales and Correlations in a Turbulent Boundary Layer," *Phys. Fluids* 15, 1545–1554 (1972).
[64] S.T. Paiziz and W.H. Schwarz, "An Investigation of the Topography and Motion of the Turbulent Interface," *J. Fluid Mech*. 63, 315–343 (1974).

[65] K.R. Sreenivasan, R. Ramshankar, and C. Meneveau, "Mixing, Entrainment and Fractal Dimensions of Surfaces in Turbulent Flows," *Proc. R. Soc. Lond. A* 421, 79–108 (1989).
[66] M. Zilberman, I. Wygnanski, I., and R.E. Kaplan, "Transitional Boundary Layer Spot in a Fully Turbulent Environment," *Phys. Fluids* 20, no. 10, part II, S258–S271 (1977).
[67] M.R. Head and P.R. Bandyopadhyay, "New Aspects of Turbulent Boundary-Layer Structure," *J. Fluid Mech*. 107, 297–338 (1981).
[68] R.E. Falco, "Some Comments on Turbulent Boundary Layer Structure Inferred from the Movements of a Passive Contaminant," AIAA Paper No. 74–99, New York, 1974.
[69] R.E. Falco, "Coherent Motions in the Outer Region of Turbulent Boundary Layers," *Phys. Fluids* 20, no. 10, part II, S124–S132 (1977).
[70] A.E. Perry, T.T. Lim, and E.W. Teh, "A Visual Study of Turbulent Spots," *J. Fluid Mech*. 104, 387–405 (1981).
[71] S.K. Robinson, S.J. Kline, and P.R. Spalart, "A Review of Quasi-Coherent Structures in a Numerically Simulated Turbulent Boundary Layer," NASA Technical Memorandum No. TM-102191, Washington, D.C., 1989.
[72] P.R. Spalart, "Direct Simulation of a Turbulent Boundary Layer up to $\Re_\theta = 1410$," NASA Technical Memorandum No. TM-89407, Washington, D.C., 1986.
[73] P.R. Spalart, "Direct Simulation of a Turbulent Boundary Layer up to $\Re_\theta = 1410$," *J. Fluid Mech*. 187, 61–98 (1988).
[74] S.J. Kline, and P.W. Runstadler, "Some Preliminary Results of Visual Studies of the Flow Model of the Wall Layers of the Turbulent Boundary Layer," *J. Appl. Mech*. 26, 166–170 (1959).
[75] P.W. Runstadler, S.J. Kline, and W.C. Reynolds, "An Experimental Investigation of Flow Structure of the Turbulent Boundary Layer," Department of Mechanical Engineering Report No. MD-8, Stanford University, Stanford, California, 1963.
[76] S.J. Kline,W.C. Reynolds, F.A. Schraub, and P.W. Runstadler, "The Structure of Turbulent Boundary Layers," *J. Fluid Mech*. 30, 741–773 (1967).
[77] H.T. Kim, S.J. Kline, and W.C. Reynolds, "The Production of Turbulence Near a Smooth Wall in a Turbulent Boundary Layer," *J. Fluid Mech*. 50, 133–160 (1971).
[78] G.R. Offen and S.J. Kline, "Combined Dye-Streak and Hydrogen-Bubble Visual Observations of a Turbulent Boundary Layer," *J. Fluid Mech*. 62, 223–239 (1974).
[79] G.R. Offen and S.J. Kline, "A Proposed Model of the Bursting Process in Turbulent Boundary Layers," *J. Fluid Mech*. 70, 209–228 (1975).
[80] R.F. Blackwelder, "The Bursting Process in Turbulent Boundary Layers," in *Workshop on Coherent Structure of Turbulent Boundary Layers*, eds. C.R. Smith and D.E. Abbott, pp. 211–227, Lehigh University, Bethlehem, Pennsylvania, 1978.
[81] R.F. Blackwelder and H. Eckelmann, "Streamwise Vortices Associated with the Bursting Phenomenon," *J. Fluid Mech*. 94, 577–594 (1979).
[82] P.G. Saffman and G.R. Baker, "Vortex Interactions," *Annu. Rev. Fluid Mech*. 11, 95–122 (1979).
[83] C.R. Smith and S.P. Schwartz, "Observation of Streamwise Rotation in the Near-Wall Region of a Turbulent Boundary Layer," *Phys. Fluids* 26, 641–652 (1983).
[84] S. Corrsin, "Some Current Problems in Turbulent Shear Flow," in *Symp. on Naval Hydrodynamics*, ed. F.S. Sherman, pp. 373–400, National Academy of Sciences/National Research Council Publication No. 515, Washington, D.C., 1957.
[85] C.R. Smith and S.P. Metzler, "The Characteristics of Low-Speed Streaks in the Near-Wall Region of a Turbulent Boundary Layer," *J. Fluid Mech*. 129, 27–54 (1983).
[86] J. Kim, P. Moin, and R.D. Moser, "Turbulence Statistics in Fully-Developed Channel Flow at Low Reynolds Number," *J. Fluid Mech*. 177, 133–166 (1987).
[87] K.M. Butler and B.F. Farrell, "Optimal Perturbations and Streak Spacing in Wall-Bounded Shear Flow," *Phys. Fluids* A 5, 774–777 (1993).
[88] J.D. Swearingen and R.F. Blackwelder, "Instantaneous Streamwise Velocity Gradients in the Wall Region," *Bul. Am. Phys. Soc*. 29, p. 1528 (1984).
[89] E.R. Corino and R.S. Brodkey, "A Visual Investigation of the Wall Region in Turbulent Flow," *J. Fluid Mech*. 37, 1–30 (1969).
[90] R.E. Falco, "New Results, a Review and Synthesis of the Mechanism of Turbulence Production in Boundary Layers and Its Modification," AIAA Paper No. 83–0377, New York, 1983.
[91] R.E. Falco, "A Coherent Structure Model of the Turbulent Boundary Layer and Its Ability to Predict Reynolds Number Dependence," *Phil. Trans. R. Soc. London A* 336, 103–129 (1991).
[92] J.C. Klewicki, J.A. Murray, and R.E. Falco, "Vortical Motion Contributions to Stress Transport in Turbulent Boundary Layers," *Phys. Fluids* 6, 277–286 (1994).
[93] G.L. Donohue, W.G. Tiederman, and M.M. Reischman, "Flow Visualization of the Near-Wall Region in a Drag-Reducing Channel Flow," *J. Fluid Mech*. 56, 559–575 (1972).
[94] M.M. Reischman and W.G. Tiederman, "Laser-Doppler Anemometer Measurements in Drag-Reducing Channel Flows," *J. Fluid Mech*. 70, 369–392 (1975).
[95] D.K. Oldaker and W.G. Tiederman, "Spatial Structure of the Viscous Sublayer in Drag-Reducing Channel Flows," *Phys. Fluids* 20, no. 10, part II, S133–144 (1977).
[96] W.G. Tiederman, T.S. Luchik, and D.G. Bogard, "Wall-Layer Structure and Drag Reduction," *J. Fluid Mech*. 156, 419–437 (1985).
[97] C.R. Smith and S.P. Metzler, "A Visual Study of the Characteristics, Formation, and Regeneration of Turbulent Boundary Layer Streaks," in *Developments in Theoretical and Applied Mechanics*, vol. XI, eds. T.J. Chung and G.R. Karr, pp. 533–543, University of Alabama, Huntsville, Alabama, 1982.
[98] C.R. Smith and S.P. Metzler, "The Characteristics of Low-Speed Streaks in the Near-Wall Region of a Turbulent Boundary Layer," *J. Fluid Mech*. 129, 27–54 (1983).
[99] M. Gad-el-Hak and A.K.M.F. Hussain, "Coherent Structures in a Turbulent Boundary Layer. Part 1. Generation of 'Artificial' Bursts," *Phys. Fluids* 29, 2124–2139 (1986).
[100] M. Gad-el-Hak and R.F. Blackwelder, "Simulation of Large-Eddy Structures in a Turbulent Boundary Layer," *AIAA J*. 25, 1207–1215 (1987).
[101] M. Gad-el-Hak and P.R. Bandyopadhyay, "Reynolds Number Effects in Wall-Bounded Flows," *Appl. Mech. Rev*. 47, pp. 307–365 (1994).
[102] M. Gad-el-Hak, *Flow Control: Passive, Active, and Reactive Flow Management*, second printing, Cambridge University Press, London, 2006.
[103] K.R. Sreenivasan, "A Unified View of the Origin and Morphology of the Turbulent Boundary Layer Structure," in *Turbulence Management and Relaminarisation*, eds. H.W. Liepmann and R. Narasimha, pp. 37–61, Springer-Verlag, Berlin, 1988.

[104] X. Wu and P. Moin, "Direct Numerical Simulation of Turbulence in a Nominally Zero-Pressure-Gradient Flat-Plate Boundary Layer," *J. Fluid Mech*. 630, pp. 5–41 (2009).
[105] M. Gad-el-Hak, "DNS of Turbulent Boundary Layers: the Breakthrough That Opened a Can of Worms," *CFD Letters* 1(2), pp. ii–iv (2009).
[106] A.E. Alving, A.J. Smits, and J.H. Watmuff, "Turbulent Boundary Layer Relaxation from Convex Curvature," *J. Fluid Mech*. 211, 529–556 (1990).
[107] G.L. Brown and A.S.W. Thomas, "Large Structure in a Turbulent Boundary Layer," *Phys. Fluids* 20, no. 10, part II, S243–S252 (1997).
[108] P.R. Bandyopadhyay, "Large Structure with a Characteristic Upstream Interface in Turbulent Boundary Layers," *Phys. Fluids* 23, 2326–2327 (1980).
[109] W.W. Willmarth and B.J. Tu, "Structure of Turbulence in the Boundary Layer Near the Wall," *Phys. Fluids* 10, S134–S137 (1967).
[110] T.J. Black, "An Analytical Study of the Measured Wall Pressure Field under Supersonic Turbulent Boundary Layers," NASA Contractor Report No. CR-888, Washington, D.C., 1988.
[111] J.O. Hinze, *Turbulence*, second edition, McGraw-Hill, New York, 1975.
[112] A.K. Praturi and R.S. Brodkey, "A Stereoscopic Visual Study of Coherent Structures in Turbulent Shear Flows," *J. Fluid Mech*. 89, 251–272 (1978).
[113] A.S.W. Thomas and M. K. Bull, "On the Role of Wall- Pressure Fluctuations in Deterministic Motions in the Turbulent Boundary Layer," *J. Fluid Mech*. 128, 283–322 (1983).
[114] M.S. Acarlar and C.R. Smith, "A Study of Hairpin Vortices in a Laminar Boundary Layer. Part 1. Hairpin Vortices Generated by a Hemisphere Protuberance," *J. Fluid Mech*. 175, 1–41 (1987).
[115] M.S. Acarlar and C.R. Smith, "A Study of Hairpin Vortices in a Laminar Boundary Layer. Part 2. Hairpin Vortices Generated by Fluid Injection," *J. Fluid Mech*. 175, 43–83 (1987).
[116] S.K. Robinson, "A Review of Vortex Structures and Associated Coherent Motions in Turbulent Boundary layers," in *Structure of Turbulence and Drag Reduction*, ed. A. Gyr, pp. 23–50, Springer-Verlag, Berlin, 1990.
[117] S.J. Kline and N.H. Afgan, editors, Near-Wall Turbulence: *1988 Zoran Zarić Memorial Conference*, Hemisphere, New York, 1990.
[118] M.T. Landahl, "A Wave-Guide Model for Turbulent Shear Flow," *J. Fluid Mech*. 29, 441–459 (1967).
[119] M.T. Landahl, "A Note on an Algebraic Instability of Inviscid Parallel Shear Flows," *J. Fluid Mech*. 98, 243–251 (1980).
[120] M.T. Landahl, "On Sublayer Streaks," *J. Fluid Mech*. 212, 593–614 (1990).
[121] A.E. Perry and M.S. Chong, "On the Mechanism of Wall Turbulence," *J. Fluid Mech*. 119, 173–217 (1982).
[122] A.E. Perry, S.M. Henbest, and M.S. Chong, "A Theoretical and Experimental Study of Wall Turbulence," *J. Fluid Mech*. 165, 163–199, 1986.
[123] A.E. Perry, J.D. Li, S. Henbest, and I. Marusic, "The Attached Eddy Hypothesis in Wall Turbulence," in *Near-Wall Turbulence: 1988 Zoran Zarić Memorial Conference*, eds. S.J. Kline and N.H. Afgan, pp. 715–735, Hemisphere, New York, 1990.
[124] J.D.A.Walker and S. Herzog, "Eruption Mechanisms for Turbulent Flows Near Walls," in *Transport Phenomena in Turbulent Flows*, eds. M. Hirata and N. Kasagi, pp. 145–156, Hemisphere, New York, 1988.
[125] N. Aubry, P. Holmes, J.L. Lumley, and E. Stone, "The Dynamics of Coherent Structures in the Wall Region of a Turbulent Boundary Layer," *J. Fluid Mech*. 192, 115–173 (1988).
[126] T.J. Hanratty, "A Conceptual Model of the Viscous Wall Region," in *Near-Wall Turbulence: 1988 Zoran Zarić Memorial Conference*, eds. S.J. Kline and N.H. Afgan, pp. 81–103, Hemisphere, New York, 1990.
[127] G. Berkooz, P. Holmes, and J.L. Lumley, "Intermittent Dynamics in Simple Models of the Turbulent Boundary Layer," *J. Fluid Mech*. 230, 75–95 (1991).
[128] W.V.R. Malkus, "Outline of a Theory of Turbulent Shear Flow," *J. Fluid Mech*. 1, 521–539 (1956).
[129] W.V.R. Malkus, "Turbulent Velocity Profiles from Stability Criteria," *J. Fluid Mech*. 90, 401–414 (1979).
[130] P. Bradshaw, "'Inactive' Motion and Pressure Fluctuations in Turbulent Boundary Layers," *J. Fluid Mech*. 30, 241–258 (1967).
[131] Y. Nagano and M. Tagawa, "A Structural Turbulence Model for Triple Products of Velocity and Scalar," *J. Fluid Mech*. 215, 639–657 (1990).
[132] P.R. Bandyopadhyay, and R. Balasubramanian, "A Vortex Model for Calculating Wall Pressure Fluctuations in Turbulent Boundary Layers," in *ASME Symposium on Flow Noise Modeling, Measurement and Control*, eds. T.M. Farabee, W.L. Keith, and R.M. Lueptow, NCA-Vol. 15/FED-Vol. 168, pp. 13–24, New York, 1993.
[133] P.R. Bandyopadhyay, and R. Balasubramanian, "Vortex Reynolds Number in Turbulent Boundary Layers," *Theor. Comput. Fluid Dynamics* 7, 101–117 (1995).
[134] P.R. Bandyopadhyay, and R. Balasubramanian, "Structural Modeling of the Wall Effects of Lorentz Force," *J. Fluids Eng*. 118, 412–414 (1996).
[135] Th. Theodorsen, "Mechanism of Turbulence," *Proc. Second Midwestern Conf. on Fluid Mechanics*, pp. 1–18, Ohio State University, Columbus, Ohio, 1952.
[136] Th. Theodorsen, "The Structure of Turbulence," in *50 Jahre Grenzschichtsforschung (Ludwig Prandtl Anniversal Volume)*, eds. H. Görtler and W. Tollmien, pp. 55–62, Friedr. Vieweg und Sohn, Braunschweig, Germany, 1955.
[137] T.J. Black, "Some Practical Applications of a New Theory of Wall Turbulence," *Proc. 1966 Heat Transfer & Fluid Mechanics Institute*, eds. M.A. Saad and J.A. Miller, pp. 366–386, Stanford University Press, Stanford, California, 1966.
[138] P.S. Klebanoff, K.D. Tidstrom, and L.M. Sargent, "The Three-Dimensional Nature of Boundary Layer Instability," *J. Fluid Mech*. 12, 1–34 (1962).
[139] T.I. Williams, *The History of Invention*, Facts on File Publications, New York, 1987.
[140] R. Dennell, "The World's Oldest Spears," *Nature* 385, 27 February, 767–768 (1997).
[141] H. Thieme, "Lower Palaeolithic Hunting Spears from Germany," *Nature* 385, 27 February, p. 807 (1997).
[142] L. Prandtl, "Über Flüssigkeitsbewegung bei sehr kleiner Reibung," *Proc. Third Int. Math. Cong*., pp. 484–491, Heidelberg, Germany, 1904.
[143] G.V. Lachmann, editor, *Boundary Layer and Flow Control*, vols. 1 and 2, Pergamon Press, Oxford, Great Britain, 1961.
[144] B.S. Stratford, "An Experimental Flow With Zero Skin Friction Throughout Its Region of Pressure Rise," *J. Fluid Mech*. 5, 17–35 (1959).
[145] R.H. Liebeck, "Design of Subsonic Airfoils for High Lift," *J. aircraft* 15, pp. 547–561 (1978).

[146] J.J. Riley, M. Gad-el-Hak, and R.W. Metcalfe, "Compliant Coatings," *Annu. Rev. Fluid Mech*. 20, 393–420 (1988).
[147] M. Gad-el-Hak, "Compliant Coatings: A Decade of Progress," *Appl. Mech. Rev*. 49, no. 10, part 2, S1–S11 (1996).
[148] M.I. Hussein, M.J. Leamy, and M. Ruzzene, "Flow Stabilization by Subsurface Phonons," *Appl. Mech. Rev*. 66, 040802.1–040802.38 (2014).
[149] M.I. Hussein, S. Biringen, O.R. Bilal, and A. Kucala, "Dynamics of Phononic Materials and Structures: Historical Origins, Recent Progress, and Future Outlook," *Proc. R. Soc. Lond. A* 471, 20140928.1–20140928.19 (2015).
[150] K.J. Åström and R.M. Murray, *Feedback Systems: An Introduction for Scientists and Engineers*, Princeton University Press, Princeton, New Jersey, 2008.
[151] J. Bernat, J. Kołota, S. Stępień, and P. Superczyńska, "Suboptimal Control of Nonlinear Continues-Time Locally Positive Systems Using Input-State Linearization and SDRE Approach," *Bull. Pol. Ac.: Tech*. 66, 17–22 (2018).
[152] S.P. Wilkinson, "Interactive Wall Turbulence Control," in *Viscous Drag Reduction in Boundary Layers*, eds. D.M. Bushnell and J.N. Hefner, pp. 479–509, AIAA, Washington, D.C., 1990.
[153] K.M.M. Alshamani, J.L. Livesey, and F.J. Edwards, "Excitation of the Wall Region by Sound in Fully Developed Channel Flow," *AIAA J*. 20, 334–339 (1982).
[154] S.P. Wilkinson and R. Balasubramanian, "Turbulent Burst Control through Phase-Locked Surface Depressions," AIAA Paper No. 85–0536, New York, 1985.
[155] D.M. Nosenchuck and M.K. Lynch, "The Control of Low-Speed Streak Bursting in Turbulent Spots," AIAA Paper No. 85- 0535, New York, 1985.
[156] K.S. Breuer, J.H. Haritonidis, and M.T. Landahl, "The Control of Transient Disturbances in a Flat Plate Boundary Layer through Active Wall Motion," *Phys. Fluids A* 1, 574–582 (1989).
[157] A. Kwong and A. Dowling, "Active Boundary Layer Control in Diffusers," AIAA Paper No. 93–3255, Washington, D.C., 1993.
[158] W.C. Reynolds, "Sensors, Actuators, and Strategies for Turbulent Shear-Flow Control," invited oral presentation at *AIAA Third Flow Control Conference*, 6–9 July, Orlando, Florida, 1993.
[159] J. Jacobs, R. James, C. Ratliff, and A. Glazer, "Turbulent Jets Induced by Surface Actuators," AIAA Paper No. 93–3243, Washington, D.C., 1993.
[160] S.A. Jacobson and W.C. Reynolds, "Active Control of Boundary Layer Wall Shear Stress Using Self-Learning Neural Networks," AIAA Paper No. 93–3272, AIAA, Washington, D.C., 1993.
[161] S.A. Jacobson and W.C. Reynolds, "Active Boundary Layer Control Using Flush-Mounted Surface Actuators," *Bul. Am. Phys. Soc*. 38, p. 2197, (1993).
[162] S.A. Jacobson and W.C. Reynolds, "Active Control of Transition and Drag in Boundary Layers," *Bul. Am. Phy. Soc*. 39, p. 1894 (1994).
[163] S.A. Jacobson and W.C. Reynolds, "An Experimental Investigation Towards the Active Control of Turbulent Boundary Layers," Department of Mechanical Engineering Report No. TF-64, Stanford University, Stanford, California, 1995.
[164] S.A. Jacobson and W.C. Reynolds, "Active Control of Streamwise Vortices and Streaks in Boundary Layers," *J. Fluid Mech*. 360, 179–211 (1998).
[165] X. Fan, L. Hofmann, and T. Herbert, "Active Flow Control with Neural Networks," AIAA Paper No. 93–3273, Washington, D.C., 1993.
[166] R.D. James, J.W. Jacobs, and A. Glezer, "Experimental Investigation of a Turbulent Jet Produced by an Oscillating Surface Actuator," *Appl. Mech. Rev*. 47, no. 6, part 2, S127–S1131 (1994).
[167] L.R. Keefe, "A MEMS-Based Normal Vorticity Actuator for Near-Wall Modification of Turbulent Shear Flows," *Proc. Workshop on Flow Control: Fundamentals and Practices*, eds. J.-P. Bonnet, M. Gad-el-Hak and A. Pollard, pp. 1–21, 1–5 July, Institut d'Etudes Scientifiques des Cargèse, Corsica, France, 1996.
[168] M. Gad-el-Hak, "Interactive Control of Turbulent Boundary Layers: A Futuristic Overview," *AIAA J*. 32, 1753–1765 (1994).
[169] M. Gad-el-Hak, "Modern Developments in Flow Control," *Appl. Mech. Rev*. 49, 365–379 (1996).
[170] J.L. Lumley, "Control of Turbulence," AIAA Paper No. 96-0001, Washington, D.C., 1996.
[171] J.M. McMichael, "Progress and Prospects for Active Flow Control Using Microfabricated Electromechanical Systems (MEMS)," AIAA Paper No. 96–0306, Washington, D.C., 1996.
[172] M. Mehregany, "Overview of Microelectromechanical Systems," invited oral presentation at *AIAA Third Flow Control Conference*, 6–9 July, Orlando, Florida, 1993.
[173] C.-M. Ho and Y.-C. Tai, "Review: MEMS and Its Applications for Flow Control," *J. Fluids Eng*. 118, 437–447 (1996).
[174] P.R. Bandyopadhyay, "Review–Mean Flow in Turbulent Boundary Layers Disturbed to Alter Skin Friction," *J. Fluids Eng*. 108, 127–140 (1986).
[175] J. Xu, S. Dong, M.R. Maxey, and G.E. Karniadakis, "Turbulent Drag Reduction by Constant Near-Wall Forcing," *J. Fluid Mech*. 582, 79–101 (2007).
[176] Y. Li and Y. Zhou, "Drag Reduction in a Turbulent Boundary Layer Using Periodic Blowing Through One Array of Streamwise Slits," in *Proc. 15th European Turbulence Conference*, ed. D. Lohse, tracking number 255, 25–28 August 2015.
[177] M. Gad-el-Hak and R.F. Blackwelder, "A Drag Reduction Method for Turbulent Boundary Layers," AIAA Paper No. 87–0358, New York, 1987.
[178] M. Gad-el-Hak and R.F. Blackwelder, "Selective Suction for Controlling Bursting Events in a Boundary Layer," *AIAA J*. 27, 308–314 (1989).
[179] R.F. Blackwelder and M. Gad-el-Hak, "Method and Apparatus for Reducing Turbulent Skin Friction," United States Patent No. 4,932,612, 1990.
[180] R.F. Blackwelder and J.D. Swearingen, "The Role of Inflectional Velocity Profiles inWall Bounded Flows," in *Near-Wall Turbulence: 1988 Zoran Zarić Memorial Conference*, eds. S.J. Kline and N.H. Afgan, pp. 268–288, Hemisphere, New York, 1990.
[181] J.B. Johansen and C.R. Smith, "The Effects of Cylindrical Surface Modifications on Turbulent Boundary Layers," *AIAA J*. 24, 1081–1087 (1986).
[182] S.P. Wilkinson and B.S. Lazos, "Direct Drag and Hot-Wire Measurements on Thin-Element Riblet Arrays," in *Turbulence Management and Relaminarization*, eds. H.W. Liepmann and R. Narasimha, pp. 121–131, Springer-Verlag, New York, 1987.
[183] S.P. Wilkinson, "Direct Drag Measurements on Thin-Element Riblets with Suction and Blowing," AIAA Paper No. 88-3670-CP, Washington, D.C., 1988.
[184] H. Choi, P. Moin, and J. Kim, "Active Turbulence Control for Drag Reduction inWall-Bounded Flows," *J. Fluid Mech*. 262, 75–110 (1994).

[185] P. Moin and T. Bewley, "Feedback Control of Turbulence," *Appl. Mech. Rev*. 47, no. 6, part 2, S3–S13 (1994).
[186] F. Abergel and R. Temam, "On Some Control Problems in Fluid Mechanics," *Theor. Comput. Fluid Dyn*. 1, 303–325 (1990).
[187] H. Choi, R. Temam, P. Moin, and J. Kim, "Feedback Control for Unsteady Flow and Its Application to the Stochastic Burgers Equation," *J. Fluid Mech*. 253, 509–543 (1993).
[188] T.R. Bewley, P. Moin, and R. Temam, "Optimal and Robust Approaches for Linear and Nonlinear Regulation Problems in Fluid Mechanics," AIAA Paper No. 97–1872, Reston, Virginia, 1997.
[189] T.R. Bewley, R. Temam, and M. Ziane, "A General Framework for Robust Control in Fluid Mechanics," Center for Turbulence Research No. CTR-Manuscript-169, Stanford University, Stanford, California, 1998.
[190] S.S. Sritharan, editor, *Optimal Control of Viscous Flow*, SIAM, Philadelphia, Pennsylvania, 1998.
[191] J.L. Lumley, "Control of the Wall Region of a Turbulent Boundary Layer," in *Turbulence: Structure and Control*, ed. J.M. McMichael, pp. 61–62, 1–3 April, Ohio State University, Columbus, Ohio, 1991.
[192] J.L. Lumley, "Control of Turbulence," AIAA Paper No. 96–0001, Washington, D.C., 1996.
[193] H. Choi, P. Moin, and J. Kim, "Turbulent Drag Reduction: Studies of Feedback Control and Flow Over Riblets," Department of Mechanical Engineering Report No. TF-55, Stanford University, Stanford, California, 1992.
[194] M. Gad-el-Hak, "Frontiers of Flow Control," in *Flow Control: Fundamentals and Practices*, eds. M. Gad-el-Hak, A. Pollard and J.-P. Bonnet, pp. 109–153, Springer-Verlag, Berlin, 1998.
[195] P. Perrier, "Multiscale Active Flow Control," in *Flow Control: Fundamentals and Practices*, eds. M. Gad-el-Hak, A. Pollard and J.-P. Bonnet, pp. 275–334, Springer-Verlag, Berlin, 1998.
[196] G. Berkooz, M. Fisher, and M. Psiaki, "Estimation and Control of Models of the TurbulentWall Layer," *Bul. Am. Phys. Soc*. 38, p. 2197 (1993).
[197] M. Gad-el-Hak, "Innovative Control of Turbulent Flows," AIAA Paper No. 93–3268, Washington, D.C., 1993.
[198] D.C. Wadsworth, E.P. Muntz, R.F. Blackwelder, and G.R. Shiflett, "Transient Energy Release Pressure Driven Microactuators for Control of Wall-Bounded Turbulent Flows," AIAA Paper No. 93–3271, AIAA, Washington, D.C., 1993.
[199] J.F. Lindner and W.L. Ditto, "Removal, Suppression and Control of Chaos by Nonlinear Design," *Appl. Mech. Rev*. 48, 795–808 (1995).
[200] S.P. Banks, *Control Systems Engineering*, Prentice-Hall International, Englewood Cliffs, New Jersey, 1986.
[201] I.R. Petersen and A.V. Savkin, *Robust Kalman Filtering for Signals and Systems with Large Uncertainties*, Birkhäuser, Boston, Massachusetts, 1999.
[202] H. Górecki and M. Zaczyk, "Determination of Optimal Controllers. Comparison of Two Methods for Electric Network Chain," *Bull. Pol. Ac.: Tech*. 66, 267–273 (2018).
[203] N. Aubry, "Use of Experimental Data for an Efficient Description of Turbulent Flows," *Appl. Mech. Rev*. 43, S240–S245 (1990).
[204] Y. Pomeau and P. Manneville, "Intermittent Transition to Turbulence in Dissipative Dynamical Systems," *Commun. Math. Phys*. 74, 189–197 (1980).
[205] S.L. Brunton and B.R. Noack, "Closed-Loop Turbulence Control: Progress and Challenges," *Appl. Mech. Rev*. 67(5), 050801 (2015).
[206] R. Grappin and J. Léorat, "Lyapunov Exponents and the Dimension of Periodic Incompressible Navier–Stokes Flows: Numerical Measurements," *J. Fluid Mech*. 222, 61–94 (1991).
[207] A.E. Deane and L. Sirovich, "A Computational Study of Rayleigh-Bénard Convection. Part 1. Rayleigh-Number Scaling," *J. Fluid Mech*. 222, 231–250 (1991).
[208] L. Sirovich and A.E. Deane, "A Computational Study of Rayleigh–Bénard Convection. Part 2. Dimension Considerations," *J. Fluid Mech*. 222, 251–265 (1991).
[209] L.R. Keefe, P. Moin, and J. Kim, "The Dimension of Attractors Underlying Periodic Turbulent Poiseuille Flow," *J. Fluid Mech*. 242, 1–29 (1992).
[210] T.B. Fowler, "Application of Stochastic Control Techniques to Chaotic Nonlinear Systems," *IEEE Trans. Autom. Control* 34, 201–205 (1989).
[211] A. Hübler and E. Lüscher, "Resonant Stimulation and Control of Nonlinear Oscillators," *Naturwissenschaften* 76, 67–69 (1989).
[212] B. Huberman, "The Control of Chaos," *Proc. Workshop on Applications of Chaos*, 4–7 December, San Francisco, California, 1990.
[213] B.A. Huberman and E. Lumer, "Dynamics of Adaptive Systems," *IEEE Trans. Circuits Syst*. 37, 547–550 (1990).
[214] E. Ott, C. Grebogi, and J.A. Yorke, "Controlling Chaos," *Phys. Rev. Lett*. 64, 1196–1199 (1990).
[215] E. Ott, C. Grebogi, and J.A. Yorke, "Controlling Chaotic Dynamical Systems," in *Chaos: Soviet–American Perspectives on Nonlinear Science*, ed. D.K. Campbell, pp. 153–172, American Institute of Physics, New York, 1990.
[216] T. Shinbrot, E. Ott, C. Grebogi, and J.A. Yorke, "Using Chaos to Direct Trajectories to Targets," *Phys. Rev. Lett*. 65, 3215–3218 (1990).
[217] T. Shinbrot, W. Ditto, C. Grebogi, E. Ott, M. Spano, and J.A. Yorke, "Using the Sensitive Dependence of Chaos (the "Butterfly Effect") to Direct Trajectories in an Experimental Chaotic System," *Phys. Rev. Lett*. 68, 2863–2866 (1992).
[218] T. Shinbrot, C. Grebogi, E. Ott, and J.A. Yorke, "Using Chaos to Target Stationary States of Flows," *Phys. Lett. A* 169, 349–354, 1992.
[219] T. Shinbrot, E. Ott, C. Grebogi, and J.A. Yorke, "Using Chaos to Direct Orbits to Targets in Systems Describable by a One-Dimensional Map," *Phys. Rev. A* 45, 4165–4168 (1992).
[220] F.J. Romeiras, C. Grebogi, E. Ott, and W.P. Dayawansa, "Controlling Chaotic Dynamical Systems," *Physica D* 58, 165–192 (1992).
[221] T. Shinbrot, L. Bresler, and J.M. Ottino, "Manipulation of Isolated Structures in Experimental Chaotic Fluid Flows," *Exp. Thermal & Fluid Sci*. 16, 76–83 (1998).
[222] T. Shinbrot, C. Grebogi, E. Ott, and J.A. Yorke, "Using Small Perturbations to Control Chaos," *Nature* 363, 411–417 (1993).
[223] T. Shinbrot, "Chaos: Unpredictable Yet Controllable?" *Nonlinear Science Today* 3, 1–8 (1993).
[224] T. Shinbrot, "Progress in the Control of Chaos," *Adv. Physics* 44, 73–111 (1995).
[225] T. Shinbrot, "Chaos, Coherence and Control," in *Flow Control: Fundamentals and Practices*, eds. M. Gad-el-Hak, A. Pollard and J.-P. Bonnet, pp. 501–527, Springer-Verlag, Berlin, 1998.
[226] E. J. Kostelich, C. Grebogi, E. Ott, and J.A. Yorke, "Targeting from Time Series," *Bul. Am. Phys. Soc*. 38, p. 2194 (1993).
[227] W.L. Ditto, S.N. Rauseo, and M.L. Spano, "Experimental Control of Chaos," *Phys. Rev. Lett*. 65, 3211–3214 (1990).

[228] W.L. Ditto and L.M. Pecora, "Mastering Chaos," *Scientific American* 269, August, 78–84 (1993).
[229] A. Garfinkel, M.L. Spano, W.L. Ditto, and J.N. Weiss, "Controlling Cardiac Chaos," *Science* 257, 1230–1235 (1992).
[230] D. Auerbach, C. Grebogi, E. Ott, and J.A. Yorke, "Controlling Chaos in High Dimensional Systems," *Phys. Rev. Lett*. 69, 3479–3482 (1992).
[231] E.J. Kostelich, C. Grebogi, E. Ott, and J.A. Yorke, "Higher-Dimensional Targeting," *Phys. Rev. E* 47, 305–310 (1993).
[232] Y.-C. Lai, M. Deng, and C. Grebogi, "Controlling Hamiltonian Chaos," *Phys. Rev. E* 47, 86–92 (1993).
[233] Y.-C. Lai, T. Tél, and C. Grebogi, "Stabilizing Chaotic-Scattering Trajectories Using Control," *Phys. Rev. E* 48, 709–717 (1993).
[234] Y.-C. Lai and C. Grebogi, "Synchronization of Chaotic Trajectories Using Control," *Phys. Rev. E* 47, 2357–2360 (1993).
[235] S. Hayes, C. Grebogi, and E. Ott, "Communicating with Chaos," *Phys. Rev. Lett*. 70, 3031–3040 (1994).
[236] S. Hayes, C. Grebogi, E. Ott, and A. Mark, "Experimental Control of Chaos for Communication," *Phys. Rev. Lett*. 73, 1781–1784 (1994).
[237] Y.-C. Lai, C. Grebogi, and T. Tél, "Controlling Transient Chaos in Dynamical Systems," in *Towards the Harnessing of Chaos*, ed. M. Yamaguchi, Elsevier, Amsterdam, the Netherlands, 1994.
[238] C.-C. Chen, E. E. Wolf, and H.-C. Chang, "Low-Dimensional Spatiotemporal Thermal Dynamics on Nonuniform Catalytic Surfaces," *J. Phys. Chemistry* 97, 1055–1064 (1993).
[239] F. Qin, E.E. Wolf, and H.-C. Chang, "Controlling Spatiotemporal Patterns on a Catalytic Wafer," *Phys. Rev. Lett*. 72, 1459–1462 (1994).
[240] D. Auerbach, "Controlling Extended Systems of Chaotic Elements," *Phys. Rev. Lett*. 72, 1184–1187 (1994).
[241] L.R. Keefe, "Two Nonlinear Control Schemes Contrasted in a Hydrodynamic Model," *Phys. Fluids* A 5, 931–947 (1993).
[242] L.R. Keefe, "Drag Reduction in Channel Flow Using Nonlinear Control," AIAA Paper No. 93–3279, Washington, D.C., 1993.
[243] E. Lüscher and A. Hübler, "Resonant Stimulation of Complex Systems," *Helv. Phys. Acta* 62, 544–551 (1989).
[244] J. Singer, Y.-Z. Wang, and H.H. Bau, "Controlling a Chaotic System," *Phys. Rev. Lett*. 66, 1123–1125 (1991).
[245] Y. Wang, J. Singer, and H.H. Bau, "Controlling Chaos in a Thermal Convection Loop," *J. Fluid Mech*. 237, 479–498 (1992).
[246] J. Tang and H.H. Bau, "Stabilization of the No-Motion State in Rayleigh–Bénard Convection Through the Use of Feedback Control," *Phys. Rev. Lett*. 70, 1795–1798 (1993).
[247] J. Tang and H.H. Bau, "Feedback Control Stabilization of the No-Motion State of a Fluid Confined in a Horizontal Porous Layer Heated from Below," *J. Fluid Mech*. 257, 485–505 (1993).
[248] H.H. Hu and H.H. Bau, "Feedback Control to Delay or Advance Linear Loss of Stability in Planar Poiseuille Flow," *Proc. Roy. Soc. Lond. A* 447, 299–312 (1994).
[249] T.C. Corke, M.N. Glauser, and G. Berkooz, "Utilizing Low-Dimensional Dynamical Systems Models to Guide Control Experiments," *Appl. Mech. Rev*. 47, no. 6, part 2, S132–S138 (1994).
[250] B.D. Coller, P. Holmes, and J.L. Lumley, "Control of Bursting in Boundary Layer Models," *Appl. Mech. Rev*. 47, no. 6, part 2, S139–S143 (1994).
[251] B.D. Coller, P. Holmes, and J.L. Lumley, "Control of Noisy Heteroclinic Cycles," *Physica D* 72, 135–160 (1994).
[252] T. Shinbrot and J.M. Ottino, "Geometric Method to Create Coherent Structures in Chaotic Flows," *Phys. Rev. Lett*. 71, 843–846 (1993).
[253] T. Shinbrot and J.M. Ottino, "Using Horseshoes to Create Coherent Structures in Chaotic Fluid Flows," *Bul. Am. Phys. Soc*. 38, p. 2194 (1993).
[254] T. Shinbrot, L. Bresler, and J.M. Ottino, "Manipulation of Isolated Structures in Experimental Chaotic Fluid Flows," *Exp. Thermal & Fluid Sci*. 16, 76–83 (1998).
[255] R.R. Yager and L.A. Zadeh, editors, *An Introduction to Fuzzy Logic Applications in Intelligent Systems*, Kluwer Academic, Boston, Massachusetts, 1992.
[256] B. Bouchon-Meunier, R.R. Yager, and L.A. Zadeh, editors, *Fuzzy Logic and Soft Computing*, World Scientific, Singapore, 1995.
[257] B. Bouchon-Meunier, R.R. Yager, and L.A. Zadeh, editors, *Advances in Intelligent Computing–IPMU'94, Lecture Notes in Computer Science*, vol. 945, Springer-Verlag, Berlin, 1995.
[258] J.-S.R. Jang, C.-T. Sun, and E. Mizutani, *Neuro-Fuzzy and Soft Computing*, Prentice Hall, Upper Saddle River, New Jersey, 1997.
[259] A. Noor and C.C. Jorgensen, "A Hard Look at Soft Computing," *Aerospace America* 34, September, 34–39 (1996).
[260] J. Ouellette, "Electronic Noses Sniff Out New Markets," *Industrial Physicist* 5, no. 1, 26–29 (1999).
[261] D.E. Goldberg, *Genetic Algorithms in Search, Optimization, and Machine Learning*, Addison-Wesley, Reading, Massachusetts, 1989.
[262] L. Davis, editor, *Handbook of Genetic Algorithms*, Van Nostrand Reinhold, New York, 1991.
[263] J.H. Holland, *Adaptation in Natural and Artificial Systems*, MIT Press, Cambridge, Massachusetts, 1992.
[264] M.M. Nelson and W. T. Illingworth, *A Practical Guide to Neural Nets*, Addison-Wesley, Reading, Massachusetts, 1991.
[265] P.J. Antsaklis, "Control Theory Approach," in *Mathematical Approaches to Neural Networks*, ed. J.G. Taylor, pp. 1–23, Elsevier, Amsterdam, 1993.
[266] W.E. Faller, S.J. Schreck, and M.W. Luttges, "Real-Time Prediction and Control of Three-Dimensional Unsteady Separated Flow Fields Using Neural Networks," AIAA Paper No. 94–0532, Washington, D.C., 1994.
[267] S.J. Schreck, W.E. Faller, and M.W. Luttges, "Neural Network Prediction of Three-Dimensional Unsteady Separated Flow Fields," *J. Aircraft* 32, 178–185 (1995).
[268] M.H. Kawthar-Ali and M. Acharya, "Artificial Neural Networks for Suppression of the Dynamic-Stall Vortex over Pitching Airfoils," AIAA Paper No. 96–0540, Washington, D.C., 1996.
[269] C. Lee, C., J. Kim, D. Babcock, and R. Goodman, "Application of Neural Networks to Turbulence Control for Drag Reduction," *Phys. Fluids* 9, 1740–1747 (1997).
[270] R. King, R., ed., *Active Flow Control*, Springer-Verlag, Berlin, 2007.
[271] R. King, R., ed., *Active Flow Control II*, Springer-Verlag, Berlin, 2011.
[272] R. King, R., ed., *Active Flow and Combustion Control*, Springer-Verlag, Berlin, 2015.
[273] R. King, R., ed., *Active Flow and Combustion Control II*, Springer-Verlag, Berlin, 2019.
[274] K.S.G. Krishnan, O. Bertram, and O. Seibel, "Review of Hybrid Laminar Flow Control Systems," *Prog. Aerosp. Sci*. 93, 24–52 (2017).

[275] V.I. Kornilov and A.V. Boiko, "Advances and Challenges in Periodic Forcing of the Turbulent Boundary Layer on a Body of Revolution," *Prog. Aerosp. Sci*. 98, 57–73 (2018).
[276] J. Kim, "Control of Turbulent Boundary Layers," *Phys. Fluids* 15, 1093–1105 (2003).
[277] J. Kim, "Physics and Control of Wall Turbulence for Drag Reduction," *Phil. Trans. R. Soc. A* 369, 1396–1411 (2011).
[278] K. Iwamoto, K. Fukagata, N. Kasagi, and Y. Suzuki, "Friction Drag Reduction Achievable by Near-Wall Turbulence Manipulation at High Reynolds Number," *Phys. Fluids* 17, 011702 (2005).
[279] S. Bagheri and D.S. Henningson, "Transition Delay Using Control Theory," *Phil. Trans. R. Soc. A* 369, 1365–1381 (2011).
[280] B.A. Belson, O. Semeraro, C.W. Rowley, and D.S. Henningson, "Feedback Control of Instabilities in the Two-Dimensional Blasius Boundary Layer: The Role of Sensors and Actuators," *Phys. Fluids* 25, 054106 (2013).
[281] N. Fabbiane, O. Semeraro, S. Bagheri, and D.S. Henningson "Adaptive and Model-Based Control Theory Applied to Convectively Unstable Flows," *Appl. Mech. Rev*. 66, 060801 (2014).
[282] B.J. McKeon, "The Engine Behind (Wall) Turbulence: Perspectives on Scale Interactions," *J. Fluid Mech*. 817, P1.1–P1.86 (2017).
[283] J. Jiménez, "Coherent Structures in Wall-Bounded Turbulence," *J. Fluid Mech*. 842, P1.1–P1.100 (2018).
[284] D. Büche, P. Stoll, R. Dornberger, and P. Koumoutsakos, "Multiobjective Evolutionary Algorithm for the Optimization of Noisy Combustion Processes," *IEEE T. Syst. Man Cy. C* 32, 460–473 (2002).
[285] N. Hansen, S.D. Müller, and P. Koumoutsakos, "Reducing the Time Complexity of the Derandomized Evolution Strategy With Covariance Matrix Adaptation (CMA-ES)," *Evol. Comput*. 11, 1–18 (2003).
[286] T. Duriez, S.L. Brunton, and B.R. Noack, *Machine Learning Control–Taming Nonlinear Dynamics and Turbulence*, Springer International Publishing, Switzerland, 2016.
[287] B.R. Noack, "Closed-Loop Turbulence Control–From Human to Machine Learning," in *Proc. 4th Symposium on Fluid- Structure-Sound Interactions and Control*, eds. Y. Zhou, M. Kimura, G. Peng, A.D. Lucey, and L. Huang, pp. 23–32, Springer, Singapore, 2017.